Covariant $\bar{\mu}$-scheme effective dynamics, mimetic gravity, and nonsingular black holes: Applications to spherically symmetric quantum gravity

Muxin Han[1,†] and Hongguang Liu[2,*]

[1]*Department of Physics, Florida Atlantic University, 777 Glades Road, Boca Raton, Florida 33431-0991, USA*

[2]*Department Physik, Institut für Quantengravitation, Theoretische Physik III, Friedrich-Alexander Universität Erlangen-Nürnberg, Staudtstr. 7/B2, 91058 Erlangen, Germany*

(Received 7 July 2023; accepted 20 March 2024; published 15 April 2024)

We propose a new $\bar{\mu}$-scheme Hamiltonian effective dynamics in the spherical symmetric spacetime which is generally covariant as derived from a covariant Lagrangian. The Lagrangian belongs to the class of extended mimetic gravity Lagrangians in four dimensions. We apply the effective dynamics to both cosmology and black hole. The effective dynamics reproduces the nonsingular loop-quantum-cosmology effective dynamics. From the effective dynamics, we obtain the nonsingular black hole solution, which has a killing symmetry in addition to the spherical symmetry and reduces to the Schwarzschild geometry asymptotically near the infinity. The black hole spacetime resolves the classical singularity and approaches asymptotically the Nariai geometry $\mathrm{dS}_2 \times S^2$ at the future infinity in the interior of the black hole. The resulting black hole spacetime has the complete future null infinity $\mathscr{I}^+$. Thanks to the general covariance, the effective dynamics can be reformulated in the light cone gauge.

DOI: 10.1103/PhysRevD.109.084033

I. INTRODUCTION

The effective dynamics of quantum gravity is an interesting approach to extracting physical predictions of quantum gravity without involving noncommutativity of quantum-geometry operators. The effective dynamics is described by c-number gravity and matter fields satisfying certain differential equations modifying the Einstein equation, while the quantum gravity effects are incorporated by the modification. Some remarkable progress has been made by the effective dynamics for the symmetry reduced models in loop quantum gravity (LQG), such as loop quantum cosmology (LQC) and quantum black holes, which both the big bang and black-hole singularities are shown to be resolved, see e.g. [1–28]. The effective dynamics of quantum gravity closely relates to the program of modified gravity (see e.g. [29–31]). The modified gravity theories define the Lagrangian that modifies the Einstein-Hilbert Lagrangian by adding the higher derivative corrections. The equations of motion from the modified gravity Lagrangian gives the modified Einstein equation, which connects to the effective dynamics of quantum gravity when we relate the higher derivative corrections to the quantum gravity effect (see e.g. [32–41]).

In the effective dynamics of LQG, the modification of the Einstein equation is given by the so-called holonomy correction. Namely, the basic variables of the effective dynamics include the holonomy of the Ashtekar-Barbero connection, which is responsible for the correction to the classical Einstein equation. The classical Einstein equation is recovered only by linearizing the holonomy. The holonomy correction is of the higher derivative type, because it contains the higher orders in the connection, which is the derivative of the metric. The effective dynamics of LQG is mostly formulated in the canonical formulation based on a $3+1$ decomposition. It is often not manifest whether the effective dynamics is covariant or relying on the special foliation, and whether the dynamics is free of the Lorentz violation. Indeed, there is the long-standing debate in the LQG community about the covariance of the effective dynamics [42–46]. The effective dynamics of isotropic LQC has been shown to be covariant, because it can be derived from a covariant scalar tensor Lagrangian belonging to the extended mimetic gravity family [37,39,47–49] (see also [50] for a different approach).[1] The recent debate largely focuses on the effective black hole models in the spherical symmetric LQG.

*Corresponding author: hongguang.liu@gravity.fau.de
†hanm@fau.edu

[1]Note that the correspondence between specific mimetic theory and LQC found in [47] does not hold for anisotropic Bianchi spacetimes, as pointed out in [39].

The effective dynamics of quantum gravity is covariant if it can be derived from a manifestly covariant Lagrangian. The lesson of LQC suggests that the mimetic gravity should be a useful tool for constructing the covariant Lagrangian for the effective dynamics. Mimetic gravity is a theory of modified gravity which belongs to the family of scalar-tensor theories. The field content of the mimetic gravity contains the gravitational field $g_{\mu\nu}$ and a scalar field ϕ, as well as a Lagrangian multiplier λ. The variation of the mimetic gravity Lagrangian with respect to λ results in the mimetic constraint $\nabla_\mu\phi\nabla^\mu\phi = -1$, which implies that the constant ϕ slices are always spacelike. The (extended) mimetic gravity theory belongs to the family of degenerate higher-order scalar-tensor theories [51–53], which propagates (up to) only three degrees of freedom: one scalar and two gravity tensorial modes. It is possible to use ϕ as the clock field, whose value defines the internal time for the effective dynamics. The mimetic gravity contains higher derivative couplings between $g_{\mu\nu}$ and ϕ, which is the source of the higher derivative modification to the Einstein gravity. The initial physical motivation of the mimetic gravity has been to propose an alternative to cold dark matter in the Universe [30]. But here the mimetic gravity is viewed as an effective theory of quantum gravity.

One of the purpose of this work is to construct the covariant effective dynamics of the spherical symmetric LQG by using the mimetic gravity Lagrangian. As a result, the effective Hamiltonian H is obtained for generating the effective dynamics in the spherical symmetric sector of LQG. This Hamiltonian is of the $\bar{\mu}$-type because it is based on the $\bar{\mu}$-scheme holonomies depending on both the connection and triad. The $\bar{\mu}$-scheme holonomies are along curves with fixed Planckian length measured by the triad. Importantly, the effective Hamiltonian dynamics can be derived from the covariant mimetic gravity Lagrangian with certain prescribed higher derivative coupling. Therefore the effective dynamics is covariant thus is called the covariant $\bar{\mu}$-scheme effective dynamics. Here the Hamiltonian H is not a linear combination of constraints but a physical Hamiltonian, which relates to the internal time defined by the mimetic scalar ϕ (see [54] for some earlier discussion). Indeed the constant-ϕ slices define the foliation for the Hamiltonian effective dynamics. This foliation is a gauge fixing which make the covariance not manifest at the Hamiltonian level. But the covariance is manifest at the level of Lagrangian. The covariant mimetic gravity Lagrangian is formulated in four dimensions, and its spherical symmetry reduction results in the covariant $\bar{\mu}$-scheme effective dynamics. The covariant $\bar{\mu}$-scheme effective dynamics is a two-dimensional field theory relating to the mimetic extension of dilaton-gravity models.

It may be more precise to call the mimetic gravity Lagrangian a covariant *extension* of the $\bar{\mu}$-scheme Hamiltonian effective dynamics, because the $\bar{\mu}$-scheme Hamiltonian is only defined on constant-ϕ slices [55,56]. In this paper, we show that this mimetic-gravity extension is unique (i.e. the mimetic potential L_ϕ uniquely determined), assuming that L_ϕ depends on only two variables χ_1, χ_2 (see Sec. II). The uniqueness with the assumption on L_ϕ relaxed would need to go beyond the spherical symmetric sector.

This work may be seen as a continuation from the early attempt [38], as well as the nonsingular black hole model from the limiting curvature hypothesis [40]. The covariant $\bar{\mu}$-scheme effective dynamics proposed here has the following advantage comparing to the earlier models: The Hamiltonian of spherical symmetric gravity depends on two components A_1, A_2 of the Ashtekar-Barbero connection, which gives two different $\bar{\mu}$-scheme holonomies. A true $\bar{\mu}$-scheme Hamiltonian of LQG should depend on both holonomies, rather than A_1 or A_2 itself. This requirement is satisfied by our covariant $\bar{\mu}$-scheme Hamiltonian H but is not satisfied by the earlier models.[2]

We apply the covariant $\bar{\mu}$-scheme effective dynamics to both the homogeneous-isotropic cosmology and spherical symmetric black holes. The homogeneous and isotropic symmetry recovers the effective dynamics to the $\bar{\mu}$-scheme effective dynamics in the K-quantization LQC, and thus the covariant $\bar{\mu}$-scheme effective dynamics includes the LQC effective dynamics as a subsector. The effective dynamics resolves the big bang singularity with a nonsingular bounce. In the spherical symmetric effective dynamics, we impose an additional killing symmetry and the boundary condition that the spacetime from the effective dynamics should reduces to the Schwarzschild geometry at infinity. An advantage of our approach is that both the black hole exterior and interior are treated uniformly with a single set of effective Hamiltonian equations, relating to the fact that our spherical symmetric effective dynamics is a $(1+1)$-dimensional field theory. As a result, the solution of the effective equations gives a nonsingular black hole: The solution reduces to the Schwarzschild geometry in the low curvature regime and replaces the classical singularity by the nonsingular Planckian curvature regime. Due to the singularity resolution, the effective dynamics extends the spacetime in the Planckian curvature regime. The spacetime approaches asymptotically to the Nariai geometry $\mathrm{dS}_2 \times S^2$ at the future infinity in the interior of the black hole (this asymptotic geometry is similar to the earlier results in [8,24]). The entire spacetime from the covariant $\bar{\mu}$-scheme effective dynamics is nonsingular and has the complete future null infinity $\mathscr{I}^+$, which contains a spacelike part corresponding to the $\mathscr{I}^+$ of dS_2 and a null part corresponding to the $\mathscr{I}^+$ of the Schwarzschild geometry.

The covariant $\bar{\mu}$-scheme effective dynamics is important conceptually because guarantees the general covariance of the effective theory. Moreover, the covariant $\bar{\mu}$-scheme is

[2]The earlier models depend on one of A_1, A_2 instead of its holonomy.

also important technically, because the formulation does not rely on the $3+1$ decomposition and can adapt to any coordinate system. In particular, the effective dynamics can be formulated in the light cone gauge, which is useful in the black hole model with null-shell collapse and null dust evaporation.

The structure of this paper is summarized as the following: Sec. II reviews the spherical symmetry reduction of LQG and the idea of $\bar{\mu}$-scheme effective dynamics. An example of the covariant $\bar{\mu}$-scheme effective Hamiltonian is introduced in this section. Section III reviews the mimetic gravity Lagrangian and equations of motion in four dimensions. Section IV discusses the spherical symmetry reduction of mimetic gravity and introduce a family of 2D mimetic-dilaton-gravity models. We also discuss the gauge fixing that leads to the foliation with constant-ϕ slices. Section V studies the Hamiltonian from the mimetic gravity and/or the mimetic-dilaton-gravity models. We propose the higher derivative interactions that lead to the covariant $\bar{\mu}$-scheme effective Hamiltonian. Section VI shows that the LQC effective dynamics can be reproduced as a subsector in the covariant $\bar{\mu}$-scheme effective dynamics. Section VII discusses the nonsingular black hole solution from the covariant $\bar{\mu}$-scheme effective dynamics. Section VIII discusses the consistency between the effective dynamics in cosmology and black hole. The consistency picks up a unique choice of free parameters in the covariant $\bar{\mu}$ scheme.

II. COVARIANT $\bar{\mu}$-SCHEME EFFECTIVE DYNAMICS OF SPHERICAL SYMMETRIC QUANTUM GRAVITY

In this section, we focus on the sector of spherical symmetrical degrees of freedom in LQG in the canonical formulation. The spacetime manifold is assumed to admit a $3+1$ decomposition $\mathscr{M}_4 \simeq \mathbb{R}\times\mathcal{S}$, where $\mathcal{S}\simeq\mathbb{R}\times S^2$. We define the spherical coordinate $\sigma=(x,\theta,\phi)$ on the spatial slice $\mathcal{S}$. The global time coordinate is denoted by t. The classical phase space for LQG has the canonical variables A_a^i, E_i^a ($i=1,2,3$, $a=x,\theta,\varphi$), where A_a^i is the Ashtekar-Barbero connection and E_i^a is the densitized triad. In spherically symmetric spacetimes, we only consider (A_a^i, E_i^a) that are invariant under rotations up to gauge transformations [6,11,12,24,57]

$$\begin{aligned} A^j\tau_j &= A_1(x)\tau_1 \mathrm{d}x + (A_2(x)\tau_2 + A_3(x)\tau_3)\mathrm{d}\theta \\ &\quad + (A_2(x)\tau_3 - A_3(x)\tau_2)\sin(\theta)\mathrm{d}\varphi + \cos(\theta)\tau_1\mathrm{d}\varphi, \\ E_j\tau^j &= E^1(x)\sin(\theta)\tau_1\partial_x + (E^2(x)\tau_2 + E^3(x)\tau_3)\sin(\theta)\partial_\theta \\ &\quad + (E^2\tau_3 - E^3\tau_2)\partial_\varphi, \end{aligned} \tag{1}$$

where $\tau_j=-\frac{i}{2}\sigma_j$ with σ_j denoting Pauli matrices. The symplectic form Ω on the phase space reduces to [58,59]

$$\begin{aligned} \Omega(\delta_1,\delta_2) &= -\frac{1}{8\pi G\beta}\int \mathrm{d}^3x\,\delta_1 A_a^j(x)\wedge\delta_2 E_j^a(x), \\ &= -\frac{1}{2G\beta}\int \mathrm{d}x[\delta_1 A_1(x)\wedge\delta_2 E^1(x) \\ &\quad + 2\delta_1 A_2(x)\wedge\delta_2 E^2(x) \\ &\quad + 2\delta_1 A_3(x)\wedge\delta_2 E^3(x)], \end{aligned} \tag{2}$$

where δ_1 and δ_2 are differentials on the phase space. The symmetry-reduced theory is an $(1+1)$-dimensional field theory with the infinite-dimensional phase space.

The SU(2) Gauss constraint is reduced to only one constraint [12,58,59]:

$$\begin{aligned} G[\lambda] = 4\pi\int \mathrm{d}x\lambda(x)[&2A_2(x)E^3(x) \\ &- 2A_3(x)E^2(x) + \partial_x E^1(x)], \end{aligned} \tag{3}$$

while other two components become trivial. $G[\lambda]$ can generate gauge transformation to make E^3 vanish, and thus we gauge fix

$$E^3(x)=0. \tag{4}$$

Correspondingly, the Gauss constraint (3) is solved for $A_3(x)$

$$A_3(x)=\frac{\partial_x E^1(x)}{2E^2(x)}. \tag{5}$$

Therefore (A_3, E^3) is removed from the canonical pairs. Following [12,24,58], we introduce

$$\begin{aligned} K_x(x) &:= \frac{1}{2\beta}A_1(x), & K_\varphi(x) &:= \frac{1}{\beta}A_2(x), \\ E^x(x) &= E^1(x), & E^\varphi(x) &= E^2(x). \end{aligned} \tag{6}$$

Recall that the Ashtekar-Barbero connection $A=\Gamma+\beta K$, the above relation between K and A are due to the vanishing Levi-Civita connection Γ for these components. K_x has been rescaled by a factor of 2 in order to make the Poisson brackets uniform.

$$\{K_j(x), E^k(x')\} = G\delta_j^k\delta(x,x'), \qquad j,k=x,\varphi. \tag{7}$$

In terms of E^x and E^φ, the spherical symmetric metric is given by

$$\begin{aligned} \mathrm{d}s^2 &= -N(t,x)^2\mathrm{d}t^2 + \frac{E^\varphi(t,x)^2}{|E^x(t,x)|}[\mathrm{d}x + N^x(t,x)\mathrm{d}t]^2 \\ &\quad + |E^x(t,x)|\mathrm{d}\Omega^2, \end{aligned} \tag{8}$$

where the angular part is given by $\mathrm{d}\Omega^2=\mathrm{d}\theta^2+\sin^2\theta\mathrm{d}\varphi^2$.

The Hamiltonian H of classical gravity reduced to the spherical symmetrical sector reads [12]

$$H_0 = \int \mathrm{d}x[N(t,x)\mathcal{C}(t,x) + N^x(t,x)\mathcal{C}_x(t,x)], \tag{9}$$

$$\mathcal{C} = \frac{1}{4G\sqrt{E^x}}\left(-\frac{2E^xE^{x\prime}E^{\varphi\prime}}{E^{\varphi 2}} + \frac{4E^xE^{x\prime\prime} + E^{x\prime 2}}{2E^\varphi} - 8E^xK_xK_\varphi - 2E^\varphi[K_\varphi^2 + 1]\right),$$

$$\mathcal{C}_x = E^\varphi K_\varphi' - K_xE^{x\prime},$$

where $E^{x\prime} = \partial_x E^x$. Both $\mathcal{C}$ and $\mathcal{C}_x$ are first-class constraints for pure gravity. However, when we couple gravity to Gaussian dust fields and formulate the theory in the reduced phase space [24,60,61] (see also [62] for coupling to nonrotational dust), the dust fields defines the material reference frame, and H_0 with $N = 1, N^x = 0$ is the physical Hamiltonian for the dust time. In this case, neither $\mathcal{C}$ nor $\mathcal{C}_x$ is a constraint.

In LQG, the $\bar{\mu}$-scheme effective dynamics is generated by the modification of H_0 in terms of the $\bar{\mu}$-scheme holonomies. In the case of the spherical symmetric quantum gravity, the $\bar{\mu}$-scheme holonomies are two types of U(1) holonomies [11,12,24,58]

$$h_x = e^{2i\bar{\mu}_xK_x} \simeq e^{\int_{e_1}\mathrm{d}xA_1}, \qquad \bar{\mu}_x = \frac{\beta\sqrt{\Delta}\sqrt{E^x}}{E^\varphi}, \tag{10}$$

$$h_\theta = e^{i\bar{\mu}_\theta K_\varphi} = e^{\int_{e_2}\mathrm{d}\theta A_2}, \qquad \bar{\mu}_\theta = \frac{\beta\sqrt{\Delta}}{\sqrt{E^x}}, \tag{11}$$

$$h_\varphi = e^{\int_{e_3}\mathrm{d}\varphi A_2\sin(\theta)} = h_\theta. \tag{12}$$

The $\bar{\mu}$-scheme holonomies h_x, h_θ, h_φ know both A and E. These holonomies are along the edges e_1, e_2, e_3 of the fixed geometrical length $\sqrt{\Delta}$ in the x, θ, φ directions. Indeed, assuming A_1 and $\bar{\mu}_x$ to be approximately constant along e_1, $e^{2i\bar{\mu}_xK_x} \simeq e^{\int_0^1 \mathrm{d}u\bar{\mu}_xA_1} = e^{\int_{e_1}\mathrm{d}xA_1}$ holds in (10), if $\int_{e_1}\mathrm{d}x\cdots = \int_0^1 \mathrm{d}u\bar{\mu}_x\cdots$, and thus the length of e_1 is fixed by $\sqrt{\Delta}$

$$\int_{e_1}\mathrm{d}x\sqrt{g_{xx}} = \int_0^1 \mathrm{d}u\bar{\mu}_x\sqrt{g_{xx}} = \sqrt{\Delta}, \tag{13}$$

where the metric $g_{\mu\nu}$ is given by (8). Similarly the length of e_1 and e_3 are also fixed by $\sqrt{\Delta}$

$$\int_{e_2}\mathrm{d}\theta\sqrt{g_{\theta\theta}} = \int_0^1 \mathrm{d}u\bar{\mu}_\theta\sqrt{g_{\theta\theta}} = \sqrt{\Delta}, \tag{14}$$

$$\int_{e_3}\mathrm{d}\varphi\sqrt{g_{\varphi\varphi}} = \int_0^1 \mathrm{d}u\bar{\mu}_\theta\sin(\theta)\sqrt{g_{\varphi\varphi}} = \sqrt{\Delta}. \tag{15}$$

In LQG, Δ is identify to the minimal nonzero eigenvalue of the area operator. A_1 and $\bar{\mu}_x$ has been assumed to be approximately constant along e_1. It means that the effective theory neglects the fluctuation of A_1 in any x interval of Planck length. The modification of H_0 in terms of the $\bar{\mu}$-scheme holonomies is often called the $\bar{\mu}$-scheme polymerization. The modified Hamiltonian is called $\bar{\mu}$-scheme effective Hamiltonian.

The simplest $\bar{\mu}$-scheme effective Hamiltonian, denoted by H_{simple}, is obtained by applying the following simple replacement rule to $\mathcal{C}$ [11,24]

$$K_\varphi \to \frac{\sqrt{E^x}}{\beta\sqrt{\Delta}}\sin\left[\frac{\beta\sqrt{\Delta}}{\sqrt{E^x}}K_\varphi\right],$$
$$K_x \to \frac{E^\varphi}{2\beta\sqrt{\Delta}\sqrt{E^x}}\sin\left[\frac{\beta\sqrt{\Delta}\sqrt{E^x}}{E^\varphi}2K_x\right]. \tag{16}$$

The resulting H_{simple} (with $N = 1, N^x = 0$) as the physical Hamiltonian on the reduced phase space has been studied extensively in [24]. H_{simple} relates to the full SU(2) theory by

$$H_{\mathrm{simple}} = \frac{2}{\beta^2\kappa\Delta}\int \mathrm{d}^3x\sum_{j,k}e(\square_{jk})\mathrm{Tr}\left(h_\Delta(\square_{jk})\frac{[E^j, E^k]}{\sqrt{\det(q)}}\right) + \text{terms independent of } K, \tag{17}$$

where $\square_{jk}$ denotes the plaquette of the fixed geometrical area Δ in the (j,k) plane. $e(\square_{jk})$ denotes the area element on $\square_{jk}$. $h_\Delta(\square_{jk}) = h_\Delta^{(j)}h_\Delta^{(k)}(h_\Delta^j)^{-1}(h_\Delta^{(k)})^{-1}$, $j,k = x,\theta,\varphi$, is the SU(2) loop holonomy around $\square_{jk}$. The loop holonomy regularizes the curvature of the Ashtekar-Barbero connection by $F_{jk} \simeq \frac{1}{\Delta}[h_\Delta(\square_{jk}) - 1]$. $h_\Delta^{(j)} \in \mathrm{SU}(2)$ are the representation of $h_j \in \mathrm{U}(1)$ acting on the fundamental representation of SU(2):

$$h_\Delta^{(x)} = e^{2\bar{\mu}_xK_x\tau_1}, \qquad h_\Delta^{(\theta)} = e^{\bar{\mu}_\theta K_\varphi\tau_2}, \qquad h_\Delta^{(\varphi)} = e^{\bar{\mu}_\theta K_\varphi\tau_3}. \tag{18}$$

It is manifest that $\Delta \to 0$ reduces H_{simple} to H_0 with $N = 1, N^x = 0$. The correction in H_{simple} to H_0 is called the holonomy correction. We note that this choice of holonomies h_j is not the holonomies of full SU(2) Ashtekar-Barbero connection. They are represented as belonging to U(1) subgroups in SU(2).

This paper mainly focuses on the new $\bar{\mu}$-scheme polymerization called the covariant $\bar{\mu}$-scheme polymerization. This polymerization gives the effective physical Hamiltonian H,

$$H = \int \mathrm{d}x[N(t)\mathcal{C}_\Delta(t,x) + N^x(t,x)\mathcal{C}_x(t,x)], \tag{19}$$

where the lapse function N only depends on t and $\mathcal{C}_\Delta$ reads

$$\mathcal{C}_\Delta = \frac{\sqrt{E^x}E^\varphi}{2G\beta^2\Delta}\left[\sin^2\left(\frac{2\beta\sqrt{\Delta}\sqrt{E^x}K_x}{E^\varphi}\right) - 4\sin^2\left(\frac{\beta\sqrt{\Delta}\sqrt{E^x}}{E^\varphi}K_x + \frac{\beta\sqrt{\Delta}}{2\sqrt{E^x}}K_\varphi\right)\right] + \frac{1}{4G\sqrt{E^x}}\left(-\frac{2E^xE^{x\prime}E^{\varphi\prime}}{E^{\varphi 2}} + \frac{4E^xE^{x\prime\prime} + E^{x\prime 2}}{2E^\varphi} - 2E^\varphi\right). \tag{20}$$

There exists a covariant Lagrangian behind the Hamiltonian H, so the effective dynamics generated by H is covariant. This is the reason why it is called the covariant $\bar{\mu}$ scheme. The covariant Lagrangian is the mimetic gravity Lagrangian with the prescribed higher derivative interactions. The field content in the Lagrangian includes a scalar field ϕ in addition to the gravitational field. The discussion of the mimetic gravity and the derivation of H from the Lagrangian are given in Secs. III, IV, and V. The covariant $\bar{\mu}$-scheme Hamiltonian H gives further correction in terms of the holonomies h_x, h_θ, h_φ in addition to the holonomy correction in H_{simple}. This correction is necessary to make the effective dynamics covariant.

The scalar field ϕ serves as the physical time, and correspondingly $\mathcal{C}_\Delta$ is not a constraint and H is the physical Hamiltonian after gauge fixing (for details, see Sec. IV B). This can be seen form the fact that the lapse function (19) is not a Lagrangian multiplier but only a function of t and can be fixed to 1. The fact that C_Δ does not form a closed algebra with C_x does not contradict with the covariance.

Note that the simple $\bar{\mu}$-scheme effective dynamics with H_{simple} studied in [24] is also manifestly covariant, since it is formulated in the reduced phase space and in terms of the Dirac observables. But a covariant Lagrangian is missing for H_{simple}. In contrast, H with (20) has the advantage of having a covariant Lagrangian, which turns out to be useful for going beyond the canonical formulation of the effective dynamics.

The spacetime manifold in this paper has the boundary at infinity, so the boundary conditions and boundary terms in H need to be discussed. The boundary term in terms of Ashtekar variables in the case of asymptotically flat spacetimes has been discussed in the literature, e.g. [63–65]. In the following we briefly discuss how the boundary term for H can be obtained. We set $N^x \to 0$ at the boundary. The procedure and result are similar to the discussion in [24] for H_{simple}. Indeed, when deriving equations of motions from H, the variation δH and the integration by part result in the following boundary terms:

$$N(t)\left[\frac{8\pi E^x\delta E^{x\prime}}{\kappa\sqrt{|E^x||E^\varphi|}} - \frac{8\pi E^x\delta E^\varphi|E^\varphi|E^{x\prime}}{\kappa E^{\varphi 3}\sqrt{|E^x|}}\right]. \tag{21}$$

The following boundary conditions will play the roles in our analysis:

(1) When we study the dynamics of spherical symmetric black hole in Sec. VII, we consider E^x, E^φ to behave asymptotically as the Schwarzschild geometry in the Lemaître coordinates as $x \to \infty$[3]:

$$E^x|_{\text{bdy}} \sim \left(\frac{3}{2}\sqrt{R_s}x\right)^{4/3}, \qquad E^\varphi|_{\text{bdy}} \sim \sqrt{R_s}\left(\frac{3}{2}\sqrt{R_s}x\right)^{1/3}, \tag{22}$$

where R_s is the Schwarzschild radius. The boundary condition satisfies $E^{x\prime} = 2E^\varphi$ and thus $\delta E^{x\prime} = 2\delta E^\varphi$ asymptotically. The boundary term (21) vanishes at $x \to \infty$.

(2) The Neumann boundary condition $E^{x\prime}|_{\text{bdy}} = 0$, $\delta E^{x\prime}|_{\text{bdy}} = 0$ appears in Sec. VII as $x \to -\infty$. Both terms in (21) vanish by this boundary condition.

III. MIMETIC GRAVITY IN FOUR DIMENSIONS

The mimetic gravity provides the manifestly covariant Lagrangian for the covariant $\bar{\mu}$-scheme effective Hamiltonian. The field content of the mimetic gravity has the gravity $g_{\mu\nu}$ and a scalar field ϕ, as well as a lagrangian multiplier λ. The extended mimetic gravity action on a 4-manifold $\mathscr{M}_4$ reads [38,53]

$$S[g_{\mu\nu},\phi,\lambda] = \frac{1}{8\pi G}\int_{\mathscr{M}_{44}} \mathrm{d}^4x\sqrt{-g}\left[\frac{f(\phi)}{2}\mathcal{R}^{(4)} + L_\phi(\phi,\chi_1,\ldots,\chi_p) + \lambda(\mathscr{X}+1)\right], \tag{23}$$

where

$$\mathscr{X} = \phi_\mu\phi^\mu, \qquad \chi_n \equiv \sum_{\mu_1,\ldots,\mu_n}\phi^{\mu_2}_{\mu_1}\phi^{\mu_3}_{\mu_2}\cdots\phi^{\mu_n}_{\mu_{n-1}}\phi^{\mu_1}_{\mu_n},$$
$$\phi_\mu = \nabla_\mu\phi, \qquad \phi_{\mu\nu} = \nabla_\mu\nabla_\nu\phi. \tag{24}$$

The variation with respect to λ gives the mimetic constraint

$$\delta_\lambda S = 0 \Leftrightarrow \mathscr{X} + 1 = 0. \tag{25}$$

For all ϕ satisfying the mimetic constraint, the constant ϕ surfaces are all spacelike. If the manifold $\mathscr{M}_4$ admits a

[3]The Schwarzschild spacetime in the Lemaître coordinates (t,x,θ,φ) is given by (8) with $E^x = (\frac{3}{2}\sqrt{R_s}(x-t))^{4/3}$, $E^\varphi = \sqrt{R_s}(\frac{3}{2}\sqrt{R_s}(x-t))^{1/3}$.

global foliation such that ϕ is constant on every slice, ϕ is a global time function on $\mathscr{M}_4$. Then ϕ can serve as a clock field defining the internal time of the system, similar to the situation of deparametrizing gravity by coupling to dust or scalar fields [60,66–68]. Indeed if $f(\phi)=1$ and $L_\phi(\phi,\chi_1,\ldots,\chi_p)=0$, S reduces to the case of the Einstein gravity coupled to a single component dust field (comparing to e.g. [66]).

The mimetic potential $L_\phi(\phi,\chi_1,\ldots,\chi_p)$ gives the higher-derivative coupling between $g_{\mu\nu}$ and ϕ. Here ϕ plays the dual role of (1) being the clock field and (2) modifying the Einstein gravity by adding higher-derivative interactions, which turns out to result in the covariant $\bar{\mu}$-scheme polymerization at the Hamiltonian level.

Here we make the following choice for simplification:

$$f(\phi)=1, \qquad L_\phi = L_\phi(\chi_1,\chi_2),$$
$$\chi_1=\Box\phi, \qquad \chi_2=\phi_\mu\phi^{\mu\nu}. \tag{26}$$

That L_ϕ only depends on χ_1 and χ_2 turns out to be a convenient choice for the spherical symmetric dynamics. The higher-derivation coupling in L_ϕ turns out to be responsible for the covariant $\bar{\mu}$ polymerization. As is shown below, χ_1,χ_2 relates to two independent components of extrinsic curvatures of the constant ϕ slice in the spherical symmetric spacetime. We leave L_ϕ as an arbitrary function at this moment, and its explicit expression will be determined later.

Given the above simplification, the variational principle $\delta S=0$ gives the following equations, in addition to the mimetic constraint (see e.g. [38])

$$\delta_\phi S=0,$$
$$\Leftrightarrow -2\nabla_\mu\lambda\phi^\mu+\nabla^\mu\nabla_\mu\frac{\partial L_\phi}{\partial\chi_1}+2\nabla_\mu\nabla_\nu\left(\frac{\partial L_\phi}{\partial\chi_2}\phi^{\mu\nu}\right)=0, \tag{27}$$

$$\delta_g S=0 \Leftrightarrow G_{\mu\nu}+2\lambda\phi_\mu\phi_\nu-T^\phi_{\mu\nu}=0, \tag{28}$$

where

$$T^\phi_{\mu\nu}=g_{\mu\nu}L_\phi+\left(-2\frac{\partial L_\phi}{\partial\chi_1}\nabla_{(\mu}\phi_{\nu)}+\nabla^\alpha\left[\frac{\partial L_\phi}{\partial\chi_1}(g_{\alpha\mu}\phi_\nu+g_{\alpha\nu}\phi_\mu-g_{\mu\nu}\phi_\alpha)\right]\right)$$
$$+2\left(-2\frac{\partial L_\phi}{\partial\chi_2}\phi^\alpha_\mu\phi_{\alpha\nu}+\nabla^\alpha\left[\frac{\partial L_\phi}{\partial\chi_2}(\phi_{\alpha\mu}\phi_\nu+\phi_{\alpha\nu}\phi_\mu-\phi_{\mu\nu}\phi_\alpha)\right]\right). \tag{29}$$

The trace of Eq. (28) can be used for solving λ

$$\lambda=-\frac{1}{2}(R+T^\phi), \tag{30}$$

where T^ϕ is the trace of $T^\phi_{\mu\nu}$. The equation of motion for ϕ in (27) is not independent, but is implied by the Einstein equation (28), $\nabla^\mu G_{\mu\nu}=0$, and the mimetic constraint. The independent equations from $\delta S=0$ are the mimetic constraint (25) and the Einstein equation (28) with (30) inserted.

IV. SPHERICAL SYMMETRY REDUCTION AND 2D MIMETIC-DILATON-GRAVITY MODELS

A. Symmetry reduction

In this paper, we mainly focus on gravity with spherical symmetry. We assume $\mathscr{M}_4=\mathscr{M}_2\times S^2$ and the general spherical symmetric metric reads

$$\mathrm{d}s^2=h_{ij}(t,x)\mathrm{d}x^i\mathrm{d}x^j+E^x(t,x)(\mathrm{d}\theta^2+\sin^2\theta\mathrm{d}\varphi^2). \tag{31}$$

We denote by h_{ij} the 2D metric

$$h_{ij}\mathrm{d}x^i\mathrm{d}x^j=-N(t,x)^2\mathrm{d}t^2+\frac{E^\varphi(t,x)^2}{E^x(t,x)}[\mathrm{d}x+N^x(t,x)\mathrm{d}t]^2. \tag{32}$$

The fields E^x, E^φ, N, N^x, as well as the ϕ,λ in the mimetic action, are assumed independent of θ,φ.

We introduce the dilaton field $\psi=\frac{1}{2}\log(E^x)$. The symmetry reduction of S gives the following 2D action

$$S_2=\frac{1}{4G}\int_{\mathscr{M}_2}\mathrm{d}^2x\sqrt{-h}\Big\{e^{2\psi}(R_h+2h^{ij}\partial_i\psi\partial_j\psi)+2$$
$$+e^{2\psi}[L_\phi(\chi_1,\chi_2)+\lambda(\mathscr{X}+1)]\Big\}, \tag{33}$$

where R_h is the 2D scalar curvature, and

$$\mathscr{X}=\phi_j\phi^j, \qquad \chi_1=\Box_h\phi+2h^{ij}\partial_i\psi\partial_j\phi,$$
$$\chi_2=\phi_{ij}\phi^{ij}+2[h^{ij}\partial_i\psi\partial_j\phi]^2, \tag{34}$$

Equation (34) relates χ_1,χ_2 to three 2D quantities $\Box_h\phi$, $h^{ij}\partial_i\psi\partial_j\phi$, and $\phi_{ij}\phi^{ij}$. However, we show that $\phi_{ij}\phi^{ij}=(\Box_h\phi)^2$ on the constraint surface $\mathscr{X}+1=0$, so χ_1,χ_2 are functions of only $\Box_h\phi$ and $h^{ij}\partial_i\psi\partial_j\phi$. Indeed, we check the relation $\phi_{ij}\phi^{ij}=(\Box_h\phi)^2$ explicitly in the light cone coordinate (u,v), where the 2D metric is written as

$h_{ij}\mathrm{d}x^i\mathrm{d}x^j = -e^{2\omega(u,v)}\mathrm{d}u\mathrm{d}v$. In this coordinate, $\mathscr{X}+1=0$ is solved by $e^{2\omega(u,v)} = 4\partial_v\phi\partial_u\phi$. Applying this relation to compute $\Box_h\phi$ and $\phi_{ij}\phi^{ij}$, we obtain

$$\phi_{ij}\phi^{ij} = (\Box_h\phi)^2 = \left(\frac{\partial_u\partial_v\phi}{\partial_v\phi\partial_u\phi}\right)^2. \tag{35}$$

Since both $\phi_{ij}\phi^{ij}$ and $\Box_h\phi$ are scalars, whose values are coordinate independent, the validity of the relation $\phi_{ij}\phi^{ij} = (\Box_h\phi)^2$ is coordinate independent.

We have χ_1, χ_2 as functions of two 2D quantities $\Box_h\phi$ and $h^{ij}\partial_i\psi\partial_j\phi$, in particular

$$\chi_2 = (\Box_h\phi)^2 + 2(h^{ij}\partial_i\psi\partial_j\phi)^2. \tag{36}$$

By this relation and (34), L_ϕ in the 2D action can be understood as a function of $\Box_h\phi$ and $h^{ij}\partial_i\psi\partial_j\phi$:

$$L_\phi(\chi_1,\chi_2) = L'_\phi(\Box_h\phi, h^{ij}\partial_i\psi\partial_j\phi). \tag{37}$$

Although any function $L_\phi(\chi_1,\chi_2)$ can be understood as a function of $\Box_h\phi$ and $h^{ij}\partial_i\psi\partial_j\phi$, the inverse is nontrivial, because the squares in (36) result in that solving $\Box_h\phi$ and $h^{ij}\partial_i\psi\partial_j\phi$ as functions of χ_1, χ_2 involves in square roots and nonunique solutions.

$$\begin{aligned}\Box_h\phi &= \frac{1}{3}\left(\chi_1 - \sqrt{2}\sqrt{3\chi_2-\chi_1^2}\right),\\ h^{ij}\partial_i\psi\partial_j\phi &= \frac{1}{6}\left(2\chi_1 + \sqrt{2}\sqrt{3\chi_2-\chi_1^2}\right),\end{aligned} \tag{38}$$

$$\begin{aligned}\text{or}\quad \Box_h\phi &= \frac{1}{3}\left(\chi_1 + \sqrt{2}\sqrt{3\chi_2-\chi_1^2}\right),\\ h^{ij}\partial_i\psi\partial_j\phi &= \frac{1}{6}\left(2\chi_1 - \sqrt{2}\sqrt{3\chi_2-\chi_1^2}\right).\end{aligned} \tag{39}$$

The space of $\Box_h\phi$ and $h^{ij}\partial_i\psi\partial_j\phi$ is the double cover of the space of χ_1, χ_2. So the space of functions $L_\phi(\chi_1,\chi_2)$ is not equivalent to the space of $L'_\phi(\Box_h\phi, h^{ij}\partial_i\psi\partial_j\phi)$, which is defined on the double cover.

In either 4D or 2D, we can lift the mimetic potential to the double cover of χ_1, χ_2 and consider L'_ϕ in the action instead of L_ϕ. In 2D, we have the explicit parametrization of the double cover by $\Box_h\phi$ and $h^{ij}\partial_i\psi\partial_j\phi$, so $L'_\phi = L'_\phi(\Box_h\phi, h^{ij}\partial_i\psi\partial_j\phi)$. In either 4D or 2D, the lifting recovers the lagrangian expressed in χ_1, χ_2 thus the covariance in the full mimetic theory in 4D. By this setup, the 2D action of the spherical symmetric mimetic gravity is given by

$$\begin{aligned}S_2 = \frac{1}{4G}\int_{\mathscr{M}_2}\mathrm{d}^2x\sqrt{-h}\Big\{&e^{2\psi}(R_h + 2h^{ij}\partial_i\psi\partial_j\psi) + 2\\ &+ e^{2\psi}[L'_\phi(\Box_h\phi, h^{ij}\partial_i\psi\partial_j\phi) + \lambda(\mathscr{X}+1)]\Big\}.\end{aligned} \tag{40}$$

We introduce the variables X, Y which relate $\Box_h\phi, h^{ij}\partial_i\psi\partial_j\phi$ by

$$X = -\Box_h\phi - h^{ij}\partial_i\psi\partial_j\phi, \qquad Y = -h^{ij}\partial_i\psi\partial_j\phi. \tag{41}$$

We will show later in Sec. IV B that X, Y are related to generalized velocities of E^x and E^φ. The space of functions of $\Box_h\phi, h^{ij}\partial_i\psi\partial_j\phi$ are equivalent to the space of functions of X, Y. We set

$$L'_\phi(\Box_h\phi, h^{ij}\partial_i\psi\partial_j\phi) = \tilde{L}(X,Y). \tag{42}$$

The lagrangian analysis of S_2 closely resembles the mimetic gravity in four dimensions. The follows are equations of motion from the variational principle

$$\delta_\lambda S_2 = 0 \Leftrightarrow \nabla_j\phi\nabla^j\phi + 1 = 0, \tag{43}$$

$$\delta_\phi S_2 = 0 \Leftrightarrow \Box\xi_1 - \nabla_j(\xi_2\partial^j\psi) - 2\nabla_j(\lambda e^{2\psi}\phi^j) = 0, \tag{44}$$

$$\begin{aligned}\delta_\psi S_2 = 0 &\Leftrightarrow 2e^{2\psi}[R_h - 2\partial^j\psi\partial_j\psi - 2\Box\psi + L'_\phi] - \nabla_j(\xi_2\phi^j) = 0,\\ \delta_{h^{ij}} S_2 = 0 &\Leftrightarrow e^{2\psi}[-2\nabla_i\nabla_j\psi + 2h_{ij}\Box\psi + 3h_{ij}\partial^k\psi\partial_k\psi - e^{-2\psi}h_{ij}]\\ &\quad + -2e^{2\psi}\partial_i\psi\partial_j\psi + e^{2\psi}\lambda\phi_i\phi_j - \frac{1}{2}h_{ij}e^{2\psi}L'_\phi + \xi_2\partial_{(i}\psi\partial_{j)}\phi\\ &\quad - \frac{1}{2}\{-2\xi_1\nabla_{(i}\phi_{j)} + \nabla^k[\xi_1(h_{ki}\phi_j + h_{kj}\phi_i - h_{ij}\phi_k)]\} = 0,\end{aligned} \tag{45}$$

where the covariant derivatives are in 2D, and we have defined $\xi_1 = e^{2\psi}\partial_X\tilde{L}_\phi$, $\xi_2 = e^{2\psi}\partial_Y\tilde{L}_\phi$. Equations (45) and (45) reduce the Einstein equation to 2D by spherical symmetry. Equation (44) from the variation of ϕ is again redundant, because it is implied by ∇^i acting on (45) (contracting i index) and (45), as well as the mimetic constraint.

B. Gauge fixing and foliation

Recall that the mimetic constraint implies the constant-ϕ slice is spacelike, and thus the mimetic scalar field ϕ can serve as the clock field defining the internal time. Reducing to 2D, we assume there exists a foliation $\mathscr{M}_2 \simeq \Sigma \times \mathbb{R}$, such that ϕ is constant on every 1D curve Σ. Then generally $\phi = \phi(t)$, where t is any global time function associated to the foliation. In this foliation, $\mathscr{X} + 1 = 0$ implies $\phi_j = (N, 0)$, where the lapse function $N = N(t) = \dot{\phi}(t)$ is a function of t only. We are allowed to set the time function $t = \phi$, then the lapse function $N = 1$.

The condition $\phi = \phi(t)$, as a gauge fixing for the diffeomorphism invariant in either 2D or 4D, does not restrict any physical degrees of freedom. Indeed, given any globally smooth field ϕ (in particular $\nabla_\mu \phi$ is defined globally), the foliation can always be obtained by defining the Σ to have constant ϕ. Since the equation of motion for ϕ, (27) or (44), is redundant, ϕ is only involved in the mimetic constraint and the Einstein equation. The restriction of ϕ is mild. Indeed, we can insert any $\phi = \phi(t)$ into the Einstein equation to solve for $g_{\mu\nu}$. This is also equivalent to inserting $\phi = \phi(t)$ in the action S_2 to reduce S_2 to the gauge-fixed action $\tilde{S}_2$, then performing the variation of $\tilde{S}_2$ and solving $\delta \tilde{S}_2 = 0$.

Let us derive the gauge-fixed action $\tilde{S}_2$. The gauge-fixing condition reduces Eq. (41) to the following simple relations:

$$X = \frac{\dot{E}^\varphi - (N^x E^\varphi)'}{N E^\varphi}, \qquad Y = \frac{\dot{E}^x - N^x E^{x\prime}}{2N E^x}, \tag{46}$$

The right-hand sides relate to the extrinsic curvatures of the constant-ϕ slice. In detail, we have $X = K^x_x + K^\theta_\theta, Y = K^\theta_\theta$ with $K_{ij} = \frac{1}{2}(\dot{\gamma}_{ij} - D_i N_j - D_j N_i)$ the components of extrinsic curvature and D_i being the covariant derivative compatible with the spatial metric γ_{ij} for $i = (x, \theta, \varphi)$. Equation (46) shows that X, Y are the same as the ones in [38] [see Eq. (4.29) there]. It is useful to solve for $\dot{E}^x, \dot{E}^\varphi$

$$\dot{E}^x = E^{x\prime} N^x + 2N E^x Y, \qquad \dot{E}^\varphi = (E^\varphi N^x)' + N E^\varphi X. \tag{47}$$

We insert the gauge-fixing condition $\phi = \phi(t)$ in S_2. The relations $\phi_j = (N, 0)$, (46) and (47) reduce S_2 to the following expression

$$\tilde{S}_2 = \frac{1}{2G} \int \mathrm{d}t \mathrm{d}x N E^\varphi \sqrt{E^x} \times \left\{ -[2XY - Y^2] + \tilde{L}(X, Y) + \frac{1}{2} R^{(3)} \right\}. \tag{48}$$

Here $N = \dot{\phi}(t)$ must be understood as the external field in $\tilde{S}_2$, since it is determined by the gauge-fixing condition. X, Y are understood as (46) in $\tilde{S}_2$. The dynamical fields in $\tilde{S}_2$ are E^x, E^φ, N^x. $R^{(3)}$ depends only on E^x, E^φ and their spatial derivatives

$$R^{(3)} = \frac{2E^{x\prime} E^{\varphi\prime}}{E^{\varphi 3}} - \frac{E^{x\prime 2}}{2E^x E^{\varphi 2}} - \frac{2E^{x\prime\prime}}{E^{\varphi 2}} + \frac{2}{E^x}, \tag{49}$$

and is the scalar curvature of the 3D spatial metric

$$\mathrm{d}s^2_{(3)} = \frac{(E^\varphi)^2}{E^x} \mathrm{d}x^2 + E^x (\mathrm{d}\theta^2 + \sin^2\theta \mathrm{d}\varphi^2). \tag{50}$$

One can check explicitly that the variations of $\tilde{S}_2$ with respect to the dynamical variables E^x, E^φ, N^x reproduce the same equations of motion as from variating S_2 followed by the gauge-fixing

$$\delta_{E^x, E^\varphi, N^x} \tilde{S}_2 = \delta_{E^x, E^\varphi, N^x} S_2 |_{\phi = \phi(t), \phi_j = (N, 0)}. \tag{51}$$

Namely the gauge-fixing $\phi = \phi(t)$ commutes with the variation of the action with respect to E^x, E^φ, N^x. This is a consequence from the redundancy of $\delta_\phi S_2$.

N is not dynamical in $\tilde{S}_2$, so $\delta_N S_2 = 0$ cannot be reproduced from $\tilde{S}_2$, but before the gauge-fixing, $\delta_N S_2 = 0$ is only used to solve the Lagrangian multiplier λ, while $\tilde{S}_2$ is independent of λ. It is closely related to the fact that the trace of the Einstein equation is used to solve for λ [see (30)], and there is no Hamiltonian constraint after the gauge fixing, as to be seen in a moment.

$\tilde{S}_2$ is not manifestly covariant, simply because it is based on the gauge fixing $\phi = \phi(t)$. But the equations of motion from $\tilde{S}_2$ are identical to the ones from S_2, which is manifestly generally covariant in 2D. The equations based on the foliation with $\phi = \phi(t)$ does not contradict with the fact that the theory is generally covariant.

V. HAMILTONIAN FORMULATION OF $\bar{\mu}$-SCHEME EFFECTIVE DYNAMICS

A. Legendre transformation and the construction of mimetic potential

We apply the Hamiltonian analysis to $\tilde{S}_2$. The Hamiltonian equations reduce the second order equations of motion from the Lagrangian theory to a set of first-order differential equations, which are suitable for the initial value problem.

In order to perform the Legendre transformation, we obtain the momenta conjugated to E^x, E^φ, and N^x by

$$\pi_\varphi = 2G \frac{\delta S_2'}{\delta \dot{E}^\varphi} = \sqrt{E^x} (\partial_X \tilde{L} - 2Y), \tag{52}$$

$$\pi_x = 2G \frac{\delta S_2'}{\delta \dot{E}^x} = \frac{E^\varphi}{2\sqrt{E^x}} (\partial_Y \tilde{L} - 2X + 2Y), \tag{53}$$

$$\pi_{N^x} = \frac{\delta S_2'}{\delta \dot{N}^x} = 0. \tag{54}$$

The nonvanishing Poisson brackets are

$$\{E^x(x), \pi_x(x')\} = \{E^\varphi(x), \pi_\varphi(x')\} = 2G\delta(x, x') \quad (55)$$

The vanishing π_{N^x} in (54) gives the primary constraint.

The Legrandre transformation is the inverse of (52) and (53) and expresses X, Y in terms of π_φ, π_x, and it needs the explicit expression of $\tilde{L}$. In the following, we construct $\tilde{L}$ that corresponds to the covariant $\bar{\mu}$ scheme: We introduce the following matrix notations:

$$\mathbf{p} = \begin{pmatrix} \frac{1}{\sqrt{E^x}}\pi_\varphi \\ \frac{2\sqrt{E^x}}{E^\varphi}\pi_x \end{pmatrix}, \quad \mathbf{q} = \begin{pmatrix} X \\ Y \end{pmatrix}, \quad \mathbf{A} = \begin{pmatrix} 0 & 2 \\ 2 & -2 \end{pmatrix}. \quad (56)$$

Equations (52) and (53) can be written as

$$\mathbf{p} = \nabla_{\mathbf{q}}\tilde{L} - \mathbf{A}\cdot\mathbf{q}. \quad (57)$$

We consider the linear transformation $\mathbf{B} \in \mathrm{GL}(2, \mathbb{R})$ acting on q^a

$$\mathbf{q} \mapsto \mathbf{u} = \mathbf{B}\cdot\mathbf{q}, \qquad \mathbf{B} = \begin{pmatrix} a & b \\ c & h \end{pmatrix}, \quad (58)$$

where a, b, c, h are parameters that are constant on the spacetime. Our aim is to find $\mathbf{B}$ making (52) and (53) decouple. Indeed, the transformation leads to

$$(\mathbf{B}^{-1})^T\mathbf{p} = \nabla_{\mathbf{u}}\tilde{L} - (\mathbf{B}^{-1})^T\cdot\mathbf{A}\cdot\mathbf{B}^{-1}\cdot\mathbf{u}. \quad (59)$$

Two equations in (59) decouple when $(\mathbf{B}^{-1})^T\cdot\mathbf{A}\cdot\mathbf{B}^{-1}$ is a diagonal matrix, which occurs when

$$b = a\left(-\frac{h}{c} - 1\right). \quad (60)$$

In this case, we denote the diagonals by γ_1 and γ_2

$$(\mathbf{B}^{-1})^T\cdot\mathbf{A}\cdot\mathbf{B}^{-1} = \begin{pmatrix} \gamma_1 & 0 \\ 0 & \gamma_2 \end{pmatrix}, \qquad \gamma_1 = \frac{2c}{a^2(-c-2h)}, \qquad \gamma_2 = \frac{2}{c(c+2h)}, \quad (61)$$

and we denote this by

$$(\mathbf{B}^{-1})^T\mathbf{p} = \begin{pmatrix} P_U \\ P_V \end{pmatrix}, \qquad \mathbf{u} = \begin{pmatrix} U \\ V \end{pmatrix}, \quad (62)$$

$$U = aX + a\left(-\frac{h}{c} - 1\right)Y, \qquad V = cX + hY, \quad (63)$$

$$P_U = -\frac{h\pi_\varphi}{\sqrt{E^x}a(-c-2h)} + \frac{2c\sqrt{E^x}\pi_x}{E^\varphi a(-c-2h)}, \quad (64)$$

$$P_V = -\frac{2\sqrt{E^x}\pi_x}{E^\varphi(-c-2h)} + \frac{\pi_\varphi(\frac{h}{c}+1)}{\sqrt{E^x}(c+2h)}. \quad (65)$$

The transformation from $(\mathbf{q}, \mathbf{p})$ to (U, V, P_U, P_V) is a 4×4 symplectic matrix. The transformation results in that Eq. (59) becomes decoupled

$$P_U = \partial_U\tilde{L} - \gamma_1 U, \qquad P_V = \partial_V\tilde{L} - \gamma_2 V. \quad (66)$$

In the limit that the higher-derivative coupling in the mimetic action is turned off: $\tilde{L} \to 0$, we have

$$P_U \to -\gamma_1 U, \qquad P_V \to -\gamma_2 V. \quad (67)$$

These relates are deformed when turning on nontrivial $\tilde{L}$. Given any expressions of P_U, P_V as functions of U, V, $\tilde{L}$ can be constructed (up to integration constants) by solving (66). The covariant $\bar{\mu}$-scheme effective dynamics corresponds to

$$\begin{aligned} P_U &= \frac{\sin^{-1}(-2\gamma_1\alpha_1\sqrt{\Delta}U)}{2\alpha_1\sqrt{\Delta}} \\ &= \frac{\sin^{-1}(-2\gamma_1\alpha_1\sqrt{\Delta}(aX + a(-\frac{h}{c}-1)Y))}{2\alpha_1\sqrt{\Delta}}, \\ P_V &= \frac{\sin^{-1}(-2\gamma_2\alpha_2\sqrt{\Delta}V)}{2\alpha_2\sqrt{\Delta}} \\ &= \frac{\sin^{-1}(-2\gamma_2\alpha_2\sqrt{\Delta}(cX + hY))}{2\alpha_2\sqrt{\Delta}}, \end{aligned} \quad (68)$$

where α_1, α_2 are free parameters that are constant on the spacetime, and the factor of 2 is conventional. When we relate the construction to LQG, Δ should relate to the minimal nonzero eigenvalue in the LQG area spectrum. From the perspective of mimetic gravity, Δ is the coupling constant for the higher-derivative couplings in $\tilde{L}$. The limit (67) is recovered by $\Delta \to 0$. The expression of $\tilde{L}$ is obtained by solving (66) and requiring $\lim_{\Delta\to 0}\tilde{L} = 0$:

$$\tilde{L}(U, V) = L_1(U) + L_2(V), \quad (69)$$

$$L_1(U) = \frac{1}{4\alpha_1^2\gamma_1\Delta} - \frac{\sqrt{1 - 4\alpha_1^2\gamma_1^2\Delta U^2}}{4\alpha_1^2\gamma_1\Delta} + \frac{\gamma_1 U^2}{2} - \frac{U\sin^{-1}(2\alpha_1\gamma_1\sqrt{\Delta}U)}{2\alpha_1\sqrt{\Delta}}, \quad (70)$$

$$L_2(V) = \frac{1}{\beta^2\gamma_2\Delta} - \frac{\sqrt{1 - \beta^2\gamma_2^2\Delta V^2}}{\beta^2\gamma_2\Delta} + \frac{\gamma_2 V^2}{2} - \frac{V\sin^{-1}(2\alpha_2\gamma_2\sqrt{\Delta}V)}{2\alpha_2\sqrt{\Delta}}. \quad (71)$$

$\tilde{L}(X, Y)$ is obtained by applying the relation (63).

The inverse of (68) gives

$$\gamma_1 U = -\frac{\sin(2\alpha_1\sqrt{\Delta}P_U)}{2\alpha_1\sqrt{\Delta}},$$
$$\gamma_2 V = -\frac{\sin(2\alpha_2\sqrt{\Delta}P_V)}{2\alpha_2\sqrt{\Delta}} \tag{72}$$

The Legandre transformation as the inverse of (52) and (53) is obtained by applying the relations (63)–(65).

As a remark, $\tilde{L}$ may be defined as a multivalued function by replacing $\sin^{-1}$ in $L_1(U)$ and $L_2(V)$ by $\sin^{-1}_{(k)}$ and $\sin^{-1}_{(m)}$ $(k, m \in \mathbb{Z})$, respectively. $\sin^{-1}_{(k)}$ is defined by

$$\sin^{-1}_{(k)}(\psi) = (-1)^k \arcsin(\psi) + k\pi \in \left[-\frac{\pi}{2}+k\pi, \frac{\pi}{2}+k\pi\right], \quad k\in\mathbb{Z}, \quad \psi\in[-1,1]. \tag{73}$$

and $\sin^{-1}_{(m)}$ is similar. The space of (π_x, π_φ) [or equivalently (P_U, P_V)] is the cover space of the space of (X, Y) [or equivalently (U, V)]. The quotient from the space of (π_x, π_φ) to the space of (X, Y) is given by the "gauge invariance"

$$P_U \sim (-1)^k P_U + \frac{k\pi}{2\alpha_1\sqrt{\Delta}}, \quad P_V \sim (-1)^m P_V + \frac{m\pi}{2\alpha_2\sqrt{\Delta}}, \tag{74}$$

with $k, m \in \mathbb{Z}$. $\tilde{L}$ is single valued on the phase space although it is multivalued in X, Y:

$$\tilde{L}(U, V, P_U, P_V) = L_1(U, P_U) + L_2(V, P_V), \tag{75}$$

$$L_1(U, P_U) = \frac{1}{4\alpha_1^2\gamma_1\Delta} - \frac{\sqrt{1-4\alpha_1^2\gamma_1^2\Delta U^2}}{4\alpha_1^2\gamma_1\Delta} + \frac{\gamma_1 U^2}{2} + P_U U, \tag{76}$$

$$L_2(V, P_V) = \frac{1}{\beta^2\gamma_2\Delta} - \frac{\sqrt{1-\beta^2\gamma_2^2\Delta V^2}}{\beta^2\gamma_2\Delta} + \frac{\gamma_2 V^2}{2} + P_V V. \tag{77}$$

B. The Hamiltonian

The primary Hamiltonian from $\tilde{S}_2$ is given by

$$H = \frac{1}{2G}\int \mathrm{d}x \left(-NE^\varphi\sqrt{E^x}\left\{\tilde{L} - [2XY - Y^2] + \frac{1}{2}R^{(3)}\right\} + \pi_x \dot{E}^x + \pi_\varphi \dot{E}^\varphi + \Lambda\pi_{N^x}\right),$$
$$= \int \mathrm{d}x (N\mathcal{C}_\Delta + N^x \mathcal{C}_x + \Lambda\pi_{N^x}), \tag{78}$$

where

$$\mathcal{C}_\Delta = \frac{1}{2G}\left(-\sqrt{E^x}E^\varphi\left\{\tilde{L} - [2XY - Y^2] + \frac{1}{2}R^{(3)}\right\} + 2YE^x\pi_x + XE^\varphi\pi_\varphi\right),$$
$$\mathcal{C}_x = \frac{1}{2G}(E^{x\prime}\pi_x - E^\varphi\pi_\phi'). \tag{79}$$

It is important that here $\mathcal{C}_\Delta$ is not a constraint since $N = \dot{\phi}(t)$ is regarded as an external field in $\tilde{S}_2$.

Expressing $\mathcal{C}_\Delta$ on the phase space gives

$$\mathcal{C}_\Delta = \frac{E^\varphi\sqrt{E^x}[c+2h]}{8c\Delta G} \times \left[\frac{a^2}{\alpha_1^2}\sin^2(\alpha_1\sqrt{\Delta}P_U) - \frac{c^2}{\alpha_2^2}\sin^2(\alpha_2\sqrt{\Delta}P_V)\right] - \frac{E^\varphi\sqrt{E^x}}{4G}\left(-\frac{2E^{x\prime\prime}}{E^{\varphi 2}} + \frac{2E^{x\prime}E^{\varphi\prime}}{E^{\varphi 3}} - \frac{E^{x\prime 2}}{2E^x E^{\varphi 2}} + 2(E^x)^{-1}\right), \tag{80}$$

where P_U, P_V are given by (64) and (65). To relate to conventions and notations in some early literatures, e.g. [11,12,24], we introduce K_x, K_φ and change variables

$$\pi_x = -2K_x \qquad \pi_\varphi = -2K_\varphi. \tag{81}$$

The Poisson brackets between K_x, K_φ and E^x, E^φ are the same as (7). P_U and P_V are given by

$$P_U = \frac{-2hK_\varphi}{\sqrt{E^x}a(c+2h)} + \frac{4c\sqrt{E^x}K_x}{E^\varphi a(c+2h)}, \tag{82}$$

$$P_V = \frac{-4\sqrt{E^x}K_x}{E^\varphi(c+2h)} + \frac{2K_\varphi(-\frac{h}{c}-1)}{\sqrt{E^x}(c+2h)}. \tag{83}$$

H is the covariant $\bar{\mu}$-scheme effective Hamiltonian of the spherical symmetric LQG. The $\bar{\mu}$-scheme holonomies can be extracted from $\sin(\alpha_1\sqrt{\Delta}P_U)$ and $\sin(\alpha_2\sqrt{\Delta}P_V)$ in $\mathcal{C}_\Delta$:

$$h_x = e^{i\frac{\sqrt{\Delta}\sqrt{E^x}}{E^\varphi}A_1}, \qquad h_\theta = h_\varphi = e^{i\frac{\sqrt{\Delta}}{\sqrt{E^x}}A_2}. \tag{84}$$

with certain choice of the parameters $a, c, h, \alpha_1, \alpha_2$. For example, a convenient choice is $a = c = 1$, $h = -1$, $\alpha_2 = 2\alpha_1 = \beta$, which leads to (20) mentioned in Sec. II. As we see in Sec. VI, the cosmological effective dynamics gives the restriction to the parameters. We are going to discuss in Sec. VIII about further restricting the parameters by other considerations.

In the limit $\Delta \to 0$ that removes higher derivative couplings, K_x, K_φ relate to the components of the extrinsic curvature of the constant-ϕ slice, and H recovers the

classical Hamiltonian of the spherical symmetry reduction of 4D gravity (9) by

$$\mathcal{C}_\Delta \to \frac{1}{4G\sqrt{E^x}}\left\{-\frac{2E^xE^{x\prime}E^{\varphi\prime}}{E^{\varphi 2}}+\frac{4E^xE^{x\prime\prime}+E^{x\prime 2}}{2E^\varphi} - 8E^xK_xK_\varphi - 2E^\varphi[K_\varphi^2+1]\right\}. \tag{85}$$

All the parameters $a, c, h, \alpha_1, \alpha_2$ disappear in the limit.

Continuing of the Hamiltonian analysis, the dynamical stability of the primary constraint $\pi_{N^x} \approx 0$ gives the diffeomorphism constraint as the secondary constraint

$$\mathcal{C}_x = -\frac{1}{G}(E^{x\prime}K_x - E^\varphi K_\varphi') \approx 0. \tag{86}$$

Furthermore we have the conservation law

$$\{\mathcal{C}_x(x), H\} \approx 0. \tag{87}$$

Thus the dynamical stability of $\mathcal{C}_x$ does not give any further constraint.

The equations of motion of the mimetic-dilation-gravity models S_2 becomes four Hamiltonian equations

$$\dot{f} = \{f, H\}, \qquad f = E^x, \quad E^\varphi, \quad K_x, \quad K_\varphi \tag{88}$$

subject to the constraint $\mathcal{C}_x = 0$. The Hamiltonian equations are partial differential equations, which are first order in t and second order in x.

VI. HOMOGENEOUS AND ISOTROPIC BOUNCING COSMOLOGY

As the first application of the equations of motion, we assume the spatial homogeneity in addition to the spherical symmetry on the spatial slices in $\mathscr{M}_4$. The assumption applies to the homogeneous-isotropic cosmology. In this cases, the metric ansatz in 4D is

$$\mathrm{d}s^2 = -\mathrm{d}t^2 + \frac{\mathfrak{a}(t)^2}{1-kx^2}\mathrm{d}x^2 + x^2\mathfrak{a}(t)^2(\mathrm{d}\theta^2+\sin^2\theta\mathrm{d}\varphi^2), \tag{89}$$

where $\mathfrak{a}(t)$ denotes the scale factor, and the spatial geometry is flat, spherical, hyperbolic for $k = 0, 1, -1$. We have set $\phi = t$ and the lapse function $N = \dot{\phi} = 1$, i.e. $\phi_\mu = (1, 0, 0, 0)$, as well as the shift vector $N^x = 0$. The same metric also applies to the Oppenheimer-Snyder model homogeneous gravitational collapse inside the black hole.

We include a massless scalar field for the discussion of cosmology. The scalar field modify $\mathcal{C}_\Delta$ and $\mathcal{C}_x$ in H by

$$\mathcal{C}_\Delta \to \mathcal{C}_\Delta + \frac{\Pi^2}{8\pi\sqrt{E^x}E^\varphi} + \frac{2\pi E^{x3/2}\Phi'^2}{E^\varphi}, \tag{90}$$

$$\mathcal{C}^x \to \mathcal{C}^x + \Pi\Phi'. \tag{91}$$

We look for the solution satisfying the symmetry to the Hamiltonian equations $\dot{f} = \{f, H\}$, where $f = E^x, E^\varphi, K_x, K_\varphi, \Phi, \Pi$ and $H = \int \mathrm{d}x\mathcal{C}_\Delta$. We insert the following ansatz in the Hamiltonian equations,

$$E^x(t,x) = x^2\mathfrak{a}(t)^2, \qquad E^\varphi(t,x) = \frac{x\mathfrak{a}(t)^2}{\sqrt{1-kx^2}}, \tag{92}$$

$$K_\varphi(t,x) = 2xK(t), \qquad K_x(t,x) = \frac{K(t)}{\sqrt{1-kx^2}}, \tag{93}$$

$$\Pi(t,x) = \frac{4\pi x^2\Pi(t)}{\sqrt{1-kx^2}}, \qquad \Phi(t,x) = \Phi(t). \tag{94}$$

The ansatz respects the symmetry and the metric (89). Inserting the ansatz reduces the Hamiltonian equations from partial differential equations to ordinary differential equations. Moreover the diffeomorphism constraint $\mathcal{C}_x = 0$ is satisfied by the ansatz.

Since the ansatz relates both E^x, E^φ to single $\mathfrak{a}(t)$ and relation both K_x, K_φ to single $K(t)$, the Hamiltonian equations give a consistency condition

$$\frac{a(2c+h)\sin(\frac{8\alpha_1\sqrt{\Delta}(c-h)K(t)}{a\mathfrak{a}(t)(c+2h)})}{\alpha_1 c} = \frac{(c-h)\sin(\frac{8\alpha_2\sqrt{\Delta}(2c+h)K(t)}{c\mathfrak{a}(t)(c+2h)})}{\alpha_2}. \tag{95}$$

The homogeneous and isotropic symmetries suppose to reduce the Hamiltonian equations to evolution equations of $\mathfrak{a}(t)$ and $K(t)$. This consistency condition must be satisfied identically without imposing any restriction to $\mathfrak{a}(t)$ and $K(t)$. Then it gives the restriction to the parameter $a, c, h, \alpha_1, \alpha_2$. Here we choose

$$a = c = 1, \qquad h = -1, \qquad \alpha_2 = 2\alpha_1. \tag{96}$$

In order to compare the equations to LQC, We consider the following change of variables from $(\mathfrak{a}, K)$ to (b, V):

$$\mathfrak{a}(t) = V(t)^{1/3}, \qquad K(t) \to \frac{b(t)V(t)^{1/3}}{2}, \tag{97}$$

where $V(t)$ is the spatial volume element. We also define

$$\beta = 2\alpha_2 = 4\alpha_1. \tag{98}$$

By the change of variables, the equations of motion reduces to the $\bar{\mu}$-scheme effective equations of LQC,

$$\dot{V}(t) = \frac{3V(t)\sin(2\beta\sqrt{\Delta}b(t))}{2\beta\sqrt{\Delta}}, \tag{99}$$

$$\dot{b}(t) = -\frac{3\sin^2(\beta\sqrt{\Delta}b(t))}{2\beta^2\Delta} - \frac{kV(t)^{4/3} + 4\pi G\Pi(t)^2}{2V(t)^2}, \quad (100)$$

$$\dot{\Phi}(t) = \frac{\Pi(t)}{V(t)}, \qquad \dot{\Pi}(t) = 0. \quad (101)$$

By define the energy density

$$\rho = -\frac{\mathcal{C}_\Delta}{4\pi E^\varphi\sqrt{E^x}} = \frac{3}{8\pi G}\left(\frac{\sin^2(\beta\sqrt{\Delta}b(t))}{\beta^2\Delta} + \frac{k}{a(t)^2}\right), \quad (102)$$

we obtain the effective Friedmann equation

$$\left(\frac{\dot{\mathfrak{a}}}{\mathfrak{a}}\right)^2(t) = \left(\frac{8\pi G\rho}{3} - \frac{k}{a(t)^2}\right) \times \left(1 - \frac{\beta^2\Delta 8\pi G}{3}\left(\rho - \frac{3k}{8\pi G a(t)^2}\right)\right). \quad (103)$$

The above equations coincide with the effective equations of LQC with the K quantization (see e.g. [69]) by identifying β to be the Barbero-Immirzi parameter. In particular, the LQC holonomy corrections given by the sine functions are reproduced by the mimetic gravity with our proposed L_ϕ.

Coming back to the choice of parameters, the condition (95) can be solved either by demanding both sides of (95) to vanish, or by equating up to sign both quantities inside and outside the sine functions. We consider the following solutions[4]

(1) $c = h$: In this case, the definition of β in (98) is replaced by $\beta = 2\alpha_2/h$.
(2) $c = -h/2$: β is defined by $\beta = 2\alpha_1/a$.
(3) $h = \frac{c(\alpha_1 c - 2\alpha_2 a)}{\alpha_2 a + \alpha_1 c}$: The above choice of parameters (96) is a special case of this solution. In this case, we define $\beta = \frac{2\alpha_2\alpha_1}{\alpha_2 a - \alpha_1 c}$ correspondingly.
(4) $h = \frac{c(\alpha_1 c + 2\alpha_2 a)}{-\alpha_2 a + \alpha_1 c}$: This flips $a \to -a$ of the above case. We have $\beta = \frac{2\alpha_2\alpha_1}{\alpha_2 a + \alpha_1 c}$ correspondingly.

These solutions with the corresponding definition of β lead to the same effective equations as (99)–(101). So all these choices are allowed for the cosmological effective dynamics. We will come back to these solutions in Sec. VIII and consider the restriction of parameter beyond the cosmological effective dynamics.

We may introduce an effective Hamiltonian H_{eff} and an effective Poisson bracket $\{,\}_{\text{eff}}$ of the homogeneous-isotropic cosmology

$$H_{\text{eff}} = -\frac{3V\sin^2(\beta\sqrt{\Delta}b)}{8\pi\beta^2\Delta G} - \frac{3kV^{1/3}}{8\pi G} + \frac{\Pi^2}{2V},$$
$$\{b, V\}_{\text{eff}} = 4\pi G, \qquad \{\Phi, \Pi\}_{\text{eff}} = 1 \quad (104)$$

H_{eff} and $\{,\}_{\text{eff}}$ coincide to the Hamiltonian and Poisson bracket in LQC. Equations (99)–(101) are equivalent to

$$\dot{f} = \{f, H_{\text{eff}}\}_{\text{eff}}, \qquad f = V, b, \Phi, \Pi. \quad (105)$$

We consider the cosmological evolution and set the initial time t_0 to be nowadays. For the initial condition, it is reasonable to assume that the mimetic scalar and higher-derivative coupling should have negligible contribution nowadays, so that the initial data $V(t_0), b(t_0), \Phi(t_0), \Pi(t_0)$ gives $H_{\text{eff}} = 0$ same as the Hamiltonian constraint. H_{eff} is conserved in the time evolution. The time evolution from the initial data gives the solution illustrated in Figs. 1(a) and 1(b). The dynamics resolves the big bang singularity with a nonsingular bounce. The bounce is symmetric in time-reversal.

Recall the Einstein equation of mimetic gravity (28). We extract the stress-energy tensor $T'_{\mu\nu} = T^\phi_{\mu\nu} + (R + T^\phi)\phi_\mu\phi_\nu$ of the mimetic field by compute the 4D Einstein tensor and applying the equations of motion:

$$G_{\mu\nu} = 8\pi G T^{\text{scalar}}_{\mu\nu} + T'_{\mu\nu}. \quad (106)$$

We still assume $H_{\text{eff}} = 0$, and we obtain

$$T^{\text{scalar}}_{\mu\nu} = (\rho_s + p_s)\phi_\mu\phi_\nu + p_s g_{\mu\nu},$$
$$\rho_s = p_s = \frac{\Pi^2}{2V^2} = \frac{3\sin^2(\beta\sqrt{\Delta}b)}{8\pi\beta^2\Delta G} + \frac{3k}{8\pi G V^{2/3}},$$
$$T'_{\mu\nu} = (\rho' + p')\phi_\mu\phi_\nu + p' g_{\mu\nu}, \qquad \rho' = -\frac{3\sin^4(\beta\sqrt{\Delta}b)}{\beta^2\Delta},$$
$$p' = -\frac{9\sin^4(\beta\sqrt{\Delta}b)}{\beta^2\Delta} - \frac{8k\sin^2(\beta\sqrt{\Delta}b)}{V^{2/3}}.$$

$T'_{\mu\nu}$ behaves effectively as a perfect fluid with the density ρ' and pressure p'. Both ρ' and p' are of $O(\Delta)$. From the viewpoint of the effective dynamics of LQG, $T'_{\mu\nu}$ is the effective stress-energy tensor counting the quantum correction to the Einstein equation, while it is also the stress-energy tensor of the mimetic field from the mimetic-gravity point of view.

The bounce is at the time t_c where

$$\dot{V}(t_c) = 0, \qquad b(t_c) = \frac{\pi}{2\beta\sqrt{\Delta}}, \quad (107)$$

we obtain the critical densities and pressures

$$\rho_s(t_c) = p_s(t_c) = \frac{3}{8\pi\beta^2\Delta G} + \frac{3k}{8\pi G V(t_c)^{2/3}}, \quad (108)$$

[4]When $2c + h \neq 0$ and $c \neq h$, Eq. (95) can be written as $\frac{\sin(\mathcal{X}\mathcal{F}(t))}{\mathcal{X}} = \frac{\sin(\mathcal{Y}\mathcal{F}(t))}{\mathcal{Y}}$, where $\frac{\alpha_1(c-h)}{a} = \mathcal{X}$, $\frac{\alpha_2(2c+h)}{c} = \mathcal{Y}$, $\frac{8\sqrt{\Delta}K(t)}{\mathfrak{a}(t)(c+2h)} = \mathcal{F}(t)$. It implies $\mathcal{X} = \pm\mathcal{Y}$, since $\mathcal{X}, \mathcal{Y}$ are t independent.

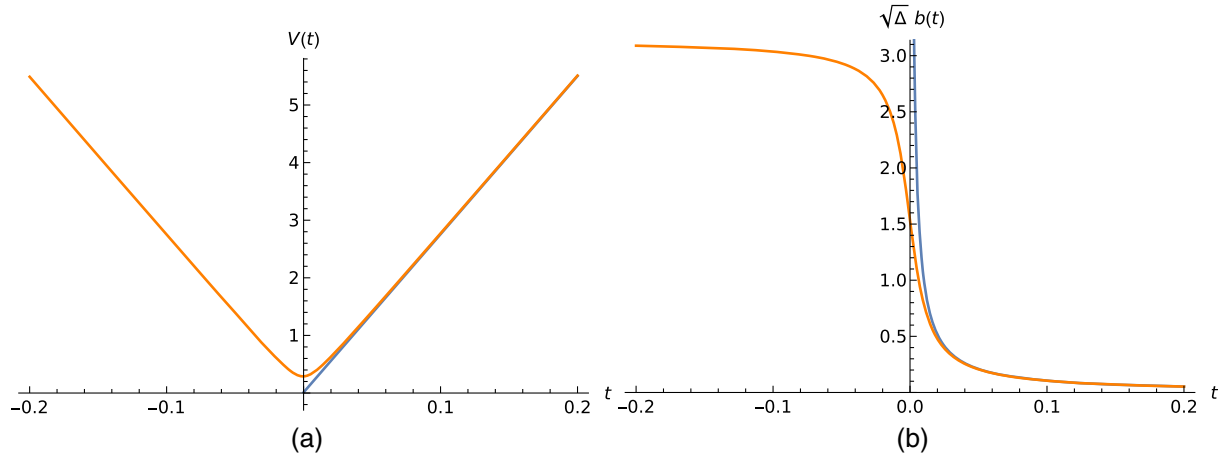

FIG. 1. The figures plot the solution (orange curves) of (99)–(101), with $k = 0$ (and $\beta = 1$), and compare to the classical FRW cosmology (blue curves). The bouncing time is at $t_c \simeq 0$.

$$\rho'(t_c) = -\frac{3}{\beta^2\Delta}, \qquad p'(t_c) = -\frac{9}{\beta^2\Delta} - \frac{8k}{V(t_c)^{2/3}}. \tag{109}$$

The Kretschmann invariant at the bounce is given by

$$\begin{aligned}\mathcal{K}(t_c) &= R_{\mu\nu\rho\sigma}(t_c)R^{\mu\nu\rho\sigma}(t_c)\\ &= \frac{108}{\beta^4\Delta^2} + \frac{60k^2}{V(t_c)^{4/3}} + \frac{144k}{\beta^2\Delta V(t_c)^{2/3}}.\end{aligned} \tag{110}$$

At the bounce, both the critical densities and the Kretschmann invariant are Planckian when $\Delta \sim \ell_P^2$ relates to the minimal nonzero eigenvalue of the LQG area operator.

Based on $\Delta \sim \ell_P^2$, the cosmic bounce is a result of the quantum effect from the LQG viewpoint. From the mimetic gravity viewpoint, the same effect is formulated as resulting from the higher-derivative coupling with the mimetic scalar ϕ. In our opinion, this two viewpoints are not contradicting but closely related. The key point is that the LQC holonomy corrections, which is responsible for the bounce, can be reproduced at the Hamiltonian level by the mimetic gravity with our proposed L_ϕ. It provides an evidence supporting our proposal that the mimetic gravity should be a candidate of the quantum effective theory for LQG, and the equations of motion of the mimetic gravity Lagrangian should capture quantum effects in LQG.

VII. NONSINGULAR SPHERICAL SYMMETRIC BLACK HOLE

A. Nonsingular black hole solution and asymptotic $dS_2 \times S^2$

We remove the assumption of the spatial homogeneity but still assume the spherical symmetry. To be consistent with the discussion of cosmology, we still use the choice of parameters (96). We still define the Barbero-Immirzi parameter by $\beta = 4\alpha_1 = 2\alpha_2$ as in cosmology.

We again choose $\phi(t) = t$ so that $N = \dot{\phi} = 1$. The Hamiltonian is given by $H = \int \mathrm{d}x\mathcal{C}_\Delta$, where

$$\begin{aligned}\mathcal{C}_\Delta = &\frac{\sqrt{E^x}E^\varphi}{2G\Delta}\left[\sin^2\left(\frac{2\beta\sqrt{\Delta}\sqrt{E^x}K_x}{E^\varphi}\right)\right.\\ &\left.-4\sin^2\left(\frac{\beta\sqrt{\Delta}\sqrt{E^x}}{E^\varphi}K_x + \frac{\beta\sqrt{\Delta}}{2\sqrt{E^x}}K_\varphi\right)\right]\\ &+\frac{1}{4G\sqrt{E^x}}\left(-\frac{2E^xE^{x\prime}E^{\varphi\prime}}{E^{\varphi 2}} + \frac{4E^xE^{x\prime\prime} + E^{x\prime 2}}{2E^\varphi} - 2E^\varphi\right),\end{aligned} \tag{111}$$

and we further fix $\beta = 1$ for the following numerical study of the equations of motion.

The Hamiltonian H generates the dynamics of the $(1+1)$D canonical fields $E^x, E^\varphi, K_x, K_\varphi$, subject to the constraint $\mathcal{C}_x = 0$. The spacetime metric is given by

$$\begin{aligned}\mathrm{d}s^2 = &-\mathrm{d}t^2 + \frac{E^\varphi(t,x)^2}{E^x(t,x)}\mathrm{d}x^2\\ &+ E^x(t,x)(\mathrm{d}\theta^2 + \sin^2\theta\mathrm{d}\varphi^2),\end{aligned} \tag{112}$$

which provides the geometrical interpretation to the solution.

The Hamiltonian can be derived from the mimetic action (40) with the corresponding mimetic potential $\tilde{L}'_\phi(\Box_h\phi, h^{ij}\partial_i\psi\partial_j\phi)$ given by

$$\begin{aligned}\tilde{L}'_\phi(\Box_h\phi, h^{ij}\partial_i\psi\partial_j\phi) &= L_1(X) - L_2(\Box_h\phi),\\ X &\equiv -\Box_h\phi - h^{ij}\partial_i\psi\partial_j\phi,\end{aligned} \tag{113}$$

$$L_1(X)=\frac{2}{\beta^2\Delta}-\frac{2\sqrt{1-\beta^2\Delta X^2}}{\beta^2\Delta}+X^2-\frac{2X\sin^{-1}(\beta\sqrt{\Delta}X)}{\beta\sqrt{\Delta}},$$
$$L_2(\Box_h\phi)=\frac{1}{2\beta^2\Delta}-\frac{\sqrt{1-4\beta^2\Delta(\Box_h\phi)^2}}{2\beta^2\Delta}+(\Box_h\phi)^2-\frac{\Box_h\phi\sin^{-1}(2\beta\sqrt{\Delta}\Box_h\phi)}{\beta\sqrt{\Delta}}.$$

The 4D version of the mimetic action (23) with the choice (26) and mimetic potential $L'_\phi(\chi_1,\chi_2)$ can be recovered from (113) by choosing the lift with the branch (38) asymptotically such that it is compatible with the Schwarzschild geometry in the Lemaître coordinates as $x\to\infty$.

We would like to study the spherical symmetric black hole solution and compare to the Schwarzschild black hole. The Schwarzschild spacetime in the Lemaître coordinates (t,x,θ,φ) is given by (112) with

$$E^x=\left(\frac{3}{2}\sqrt{R_s}(x-t)\right)^{4/3},$$
$$E^\varphi=\sqrt{R_s}\left(\frac{3}{2}\sqrt{R_s}(x-t)\right)^{1/3}, \tag{114}$$

where R_s is the Schwarzschild radius.

As the boundary condition for H, we consider E^x, E^φ to behave asymptotically as the Schwarzschild geometry in the Lemaître coordinates as $x\to\infty$:

$$E^x\sim\left(\frac{3}{2}\sqrt{R_s}x\right)^{4/3},\quad E^\varphi\sim\sqrt{R_s}\left(\frac{3}{2}\sqrt{R_s}x\right)^{1/3}, \tag{115}$$

Under this boundary condition, H does not need a boundary term to make δH well defined [24,59].

The Hamitonian equations $\partial_t f=\{f,H\}$ give a set of four partial differential equations (PDEs). The set of PDEs are first order in t and second order in x. We introduce the following change of variables in order to make the formulas compact

$$K_x=\frac{1}{8}\zeta_2 e^\xi,\qquad K_\varphi=-\frac{1}{4}(\zeta_1+\zeta_2)e^\psi,$$
$$E^\varphi=e^{\xi+\psi},\qquad E^x=e^{2\psi}. \tag{116}$$

One can check that $\zeta_1=2P_U,\zeta_2=2P_V$. The Hamiltonian equations in terms of ζ_1,ζ_2,ξ,ψ are given by

$$\dot\zeta_1=\frac{1}{2\Delta}\Big[8\Delta e^{-2\xi}\xi'\psi'-8\Delta e^{-2\xi}\psi'^2-8\Delta e^{-2\xi}\psi''+\sqrt{\Delta}\zeta_1\sin\left(\frac{\sqrt{\Delta}\zeta_2}{2}\right)+2\sqrt{\Delta}\zeta_2\sin\left(\frac{\sqrt{\Delta}\zeta_2}{2}\right)-16\cos\left(\frac{\sqrt{\Delta}\zeta_1}{4}\right)+4\cos\left(\frac{\sqrt{\Delta}\zeta_2}{2}\right)+12\Big], \tag{117}$$

$$\dot\zeta_2=\frac{1}{\Delta}\Big[-4\Delta e^{-2\xi}\xi'\psi'+2\Delta e^{-2\xi}\psi'^2+4\Delta e^{-2\xi}\psi''+2\Delta e^{-2\psi}+\sqrt{\Delta}\zeta_1\sin\left(\frac{\sqrt{\Delta}\zeta_1}{4}\right)+2\sqrt{\Delta}\zeta_2\sin\left(\frac{\sqrt{\Delta}\zeta_1}{4}\right)+4\cos\left(\frac{\sqrt{\Delta}\zeta_1}{4}\right)-\cos\left(\frac{\sqrt{\Delta}\zeta_2}{2}\right)-3\Big], \tag{118}$$

$$\dot\xi=\frac{1}{2\sqrt{\Delta}}\sin\left(\frac{\sqrt{\Delta}\zeta_2}{2}\right), \tag{119}$$

$$\dot\psi=-\frac{1}{2\sqrt{\Delta}}\left[\sin\left(\frac{\sqrt{\Delta}\zeta_2}{2}\right)+2\sin\left(\frac{\sqrt{\Delta}\zeta_1}{4}\right)\right], \tag{120}$$

where $\dot f=\partial_t f$ and $f'=\partial_x f$ for $f=\zeta_1,\zeta_2,\xi,\psi$.

To simplify the equations, we apply the following ansatz as in [24]

$$f(t,x)=f(z),\quad z=x-t,\quad f=\zeta_1,\zeta_2,\xi,\psi. \tag{121}$$

The ansatz is inspired by the Schwarzschild geometry in the Lemaître coordinates, and it assumes the killing symmetry generated by $\xi=\partial_t+\partial_x$. The ansatz reduces the PDEs to four first-order ordinary differential equations (ODEs)

$$\frac{\mathrm{d}f(z)}{\mathrm{d}z}=\mathcal{F}_f(z),\qquad f=\zeta_1,\zeta_2,\xi,\psi. \tag{122}$$

The explicit expressions of the ODEs are given below:

$$\frac{d\zeta_1}{dz} = \frac{e^{-2(\xi+\psi)}}{4\Delta(\cos(\frac{\sqrt{\Delta}\zeta_2}{2}) - \cos(\frac{\sqrt{\Delta}\zeta_1}{4}) + e^{2\xi})}\left[8e^{2(\xi+\psi)}\sin^2\left(\frac{\sqrt{\Delta}\zeta_2}{2}\right) + 16e^{2(\xi+\psi)}\sin^2\left(\frac{\sqrt{\Delta}\zeta_1}{4}\right)\right.$$
$$+ 24e^{2(\xi+\psi)}\sin\left(\frac{\sqrt{\Delta}\zeta_2}{2}\right)\sin\left(\frac{\sqrt{\Delta}\zeta_1}{4}\right) - 4e^{2(\xi+\psi)}\cos^2\left(\frac{\sqrt{\Delta}\zeta_2}{2}\right) - 12e^{2(\xi+\psi)}\cos\left(\frac{\sqrt{\Delta}\zeta_2}{2}\right) - 8e^{4\xi+2\psi}\cos\left(\frac{\sqrt{\Delta}\zeta_2}{2}\right)$$
$$+ 16e^{2(\xi+\psi)}\cos\left(\frac{\sqrt{\Delta}\zeta_1}{4}\right)\cos\left(\frac{\sqrt{\Delta}\zeta_2}{2}\right) + 32e^{4\xi+2\psi}\cos\left(\frac{\sqrt{\Delta}\zeta_1}{4}\right) - \sqrt{\Delta}\zeta_1 e^{2(\xi+\psi)}\left(2e^{2\xi}\sin\left(\frac{\sqrt{\Delta}\zeta_2}{2}\right) + \sin(\sqrt{\Delta}\zeta_2)\right.$$
$$\left. + 4\sin\left(\frac{\sqrt{\Delta}\zeta_1}{4}\right)\cos\left(\frac{\sqrt{\Delta}\zeta_2}{2}\right)\right) - 2\sqrt{\Delta}\zeta_2 e^{2(\xi+\psi)}\left(2e^{2\xi}\sin\left(\frac{\sqrt{\Delta}\zeta_2}{2}\right) + \sin(\sqrt{\Delta}\zeta_2) + 4\sin\left(\frac{\sqrt{\Delta}\zeta_1}{4}\right)\cos\left(\frac{\sqrt{\Delta}\zeta_2}{2}\right)\right)$$
$$- 8\Delta e^{2\xi}\cos\left(\frac{\sqrt{\Delta}\zeta_2}{2}\right) + e^{2\psi}\sin\left(\frac{\sqrt{\Delta}\zeta_2}{2}\right)\sin(\sqrt{\Delta}\zeta_2) + 4e^{2\psi}\sin\left(\frac{\sqrt{\Delta}\zeta_1}{4}\right)\sin(\sqrt{\Delta}\zeta_2)$$
$$\left. + 8e^{2\psi}\sin^2\left(\frac{\sqrt{\Delta}\zeta_1}{4}\right)\cos\left(\frac{\sqrt{\Delta}\zeta_2}{2}\right) - 24e^{4\xi+2\psi}\right], \tag{123}$$

$$\frac{d\zeta_2}{dz} = \frac{e^{-2(\xi+\psi)}}{4\Delta(\cos(\frac{\sqrt{\Delta}\zeta_2}{2}) - \cos(\frac{\sqrt{\Delta}\zeta_1}{4}) + e^{2\xi})}\left[-16e^{2(\xi+\psi)}\sin\left(\frac{\sqrt{\Delta}\zeta_1}{4}\right)\sin\left(\frac{\sqrt{\Delta}\zeta_2}{2}\right) + 12e^{2(\xi+\psi)}\cos\left(\frac{\sqrt{\Delta}\zeta_1}{4}\right)\right.$$
$$- 16e^{4\xi+2\psi}\cos\left(\frac{\sqrt{\Delta}\zeta_1}{4}\right) + 4e^{2(\xi+\psi)}\cos\left(\frac{\sqrt{\Delta}\zeta_2}{2}\right)\cos\left(\frac{\sqrt{\Delta}\zeta_1}{4}\right) - 4e^{2(\xi+\psi)}\cos\left(\frac{\sqrt{\Delta}\zeta_1}{2}\right) + 4e^{4\xi+2\psi}\cos\left(\frac{\sqrt{\Delta}\zeta_2}{2}\right)$$
$$+ 3e^{2(\xi+\psi)}\cos(\sqrt{\Delta}\zeta_2) - 2\sqrt{\Delta}\zeta_1 e^{2(\xi+\psi)}\left(2e^{2\xi}\sin\left(\frac{\sqrt{\Delta}\zeta_1}{4}\right) - \left(\sin\left(\frac{\sqrt{\Delta}\zeta_2}{2}\right) + 2\sin\left(\frac{\sqrt{\Delta}\zeta_1}{4}\right)\right)\cos\left(\frac{\sqrt{\Delta}\zeta_1}{4}\right)\right)$$
$$- 4\sqrt{\Delta}\zeta_2 e^{2(\xi+\psi)}\left(2e^{2\xi}\sin\left(\frac{\sqrt{\Delta}\zeta_1}{4}\right) - \sin\left(\frac{\sqrt{\Delta}\zeta_1}{2}\right) - \sin\left(\frac{\sqrt{\Delta}\zeta_2}{2}\right)\cos\left(\frac{\sqrt{\Delta}\zeta_1}{4}\right)\right) + 8\Delta e^{2\xi}\cos\left(\frac{\sqrt{\Delta}\zeta_1}{4}\right)$$
$$- 2e^{2\psi}\sin\left(\frac{\sqrt{\Delta}\zeta_1}{4}\right)\sin\left(\frac{\sqrt{\Delta}\zeta_1}{2}\right) - 4e^{2\psi}\sin\left(\frac{\sqrt{\Delta}\zeta_1}{2}\right)\sin\left(\frac{\sqrt{\Delta}\zeta_2}{2}\right) + 4e^{2\psi}\cos^3\left(\frac{\sqrt{\Delta}\zeta_1}{4}\right) - 5e^{2\psi}\cos\left(\frac{\sqrt{\Delta}\zeta_1}{4}\right)$$
$$\left. + e^{2\psi}\cos(\sqrt{\Delta}\zeta_2)\cos\left(\frac{\sqrt{\Delta}\zeta_1}{4}\right) - 8\Delta e^{4\xi} - 15e^{2(\xi+\psi)} + 12e^{4\xi+2\psi}\right], \tag{124}$$

$$\frac{d\xi}{dz} = -\frac{1}{2\sqrt{\Delta}}\sin\left(\frac{\sqrt{\Delta}\zeta_2}{2}\right), \tag{125}$$

$$\frac{d\psi}{dz} = \frac{1}{2\sqrt{\Delta}}\left[\sin\left(\frac{\sqrt{\Delta}\zeta_2}{2}\right) + 2\sin\left(\frac{\sqrt{\Delta}\zeta_1}{4}\right)\right]. \tag{126}$$

As the initial condition of the ODEs, we require that $E^x, E^\varphi, K_x, K_\varphi$ reduce asymptotically to the Schwarzschild as $z \to \infty$. By the Schwarzschild metric in the Lemaître coordinates, we have for $z = z_0 \gg 1$

$$E^x(z_0) = \left(\frac{3}{2}\sqrt{R_s}z_0\right)^{4/3},$$
$$E^\varphi(z_0) = \sqrt{R_s}\left(\frac{3}{2}\sqrt{R_s}z_0\right)^{1/3}, \tag{127}$$
$$K_x(z_0) = \frac{R_s}{3\times 2^{2/3}3^{1/3}(\sqrt{R_s}z_0)^{4/3}},$$
$$K_\varphi(z_0) = -\frac{(\frac{2}{3})^{1/3}\sqrt{R_s}}{(\sqrt{R_s}z_0)^{1/3}}. \tag{128}$$

Translating the initial condition to $\zeta_1, \zeta_2, \xi, \psi$ gives

$$\zeta_1(z_0) = \zeta_2(z_0) = \frac{4}{3z_0}, \qquad \psi(z_0) = \frac{1}{6}\log\left(\frac{81R_s^2z_0^4}{16}\right),$$
$$\xi(z_0) = \frac{1}{3}\log\left(\frac{2R_s}{3z_0}\right). \tag{129}$$

Then the set of ODEs can be solved numerically by assigning numerical values to parameters R_s, Δ, z_0 and imposing the above initial condition at z_0.

Equation (122) describes an evolution of fields in z. Although introducing z and the ansatz (121) are understood

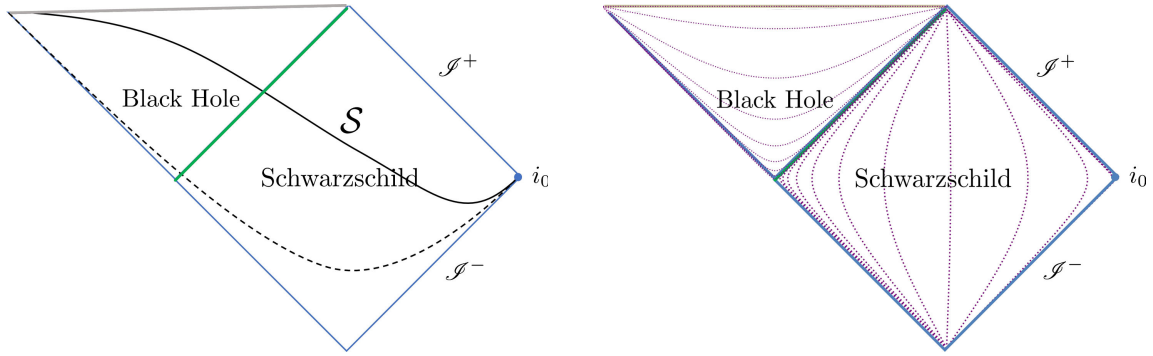

(a) Constant t slices (b) Constant z slices

FIG. 2. Illustration of constant t slices and constant z slices in Schwarzschild spacetime.

as the trick to simplify the PDEs, it is still interesting to understand the constant z slices in the spacetime and obtain a picture of the evolution. Indeed by $\xi^\mu \nabla_\mu z = 0$, the killing vector ξ is tangent to the constant z slice. The constant z slices are precisely the Kantowski-Sachs foliation commonly used in earlier studies of LQG black holes, e.g. [8,70–72]. The constant z slices is timelike in the exterior and spacelike in the interior of the black hole. See Fig. 2 for the illustration in the Schwarzschild spacetime and comparing to the constant t slices in the Lemaitre coordinates. The initial condition of the ODEs (127) and (128) are imposed on the timelike constant z slice far away from the black hole.

In the earlier work of LQG black holes with the Kantowski-Sachs foliation, one has to treat the black hole interior and exterior separately, with two different sets of effective equations. In our formulation, the evolutions in the exterior and interior are unified in one set of equations (122), since it is derived from the PDEs in the (x, t) coordinate, which covers both the exterior and interior. Moreover, the dynamics is covariant and independent of the choice of foliations, since it is derived from the manifestly covariant Lagrangian.

The set of ODEs (122) can be solved numerically with the initial condition (129). The numerical solution is computed with high numerical precision using the computing software JULIA. The resulting numerical solution satisfies the ODEs up to the maximal error bounded by $\sim 10^{-30}$ where the error is shown in Fig. 3.

The geometrical interpretation of the solution is obtained by inserting the solution in the metric (112). The spacetime geometry given by the solution has the following key features:

(1) The spacetime geometry is well approximated by the Schwarzschild geometry for large $z > 0$, and it gives corrections to the Schwarzschild spacetime as z becomes small.
(2) The black hole singularity, which happens at $z = 0$ in the Schwarzschild spacetime, is resolved. The curvature is always finite.
(3) The spacetime extends smoothly to $z < 0$ due to the singularity resolution. For negative z and large $|z|$, the spacetime approach asymptotically to the Nariai geometry $\mathrm{dS}_2 \times S^2$.

The same features also appear in the black hole effective model in [24,58], where the model is constructed by applying the simplest $\bar{\mu}$-scheme polymerization to the reduced phase space physical Hamiltonian from gravity coupled to dust.

Let us discuss in more detail about these features. In the regime of large $z > 0$, the correction to the standard Einstein gravity is negligible, and $E^x(z), E^\varphi(z), K_x(z), K_\varphi(z)$ of the solution are well approximated by (127) and (128) with z_0 replaced by z. In particular, the quantum correction at the event horizon $z_H = 2R_s/3$ is negligible for large black holes $R_s \gg \sqrt{\Delta}$. The solution gives that the marginal trapped

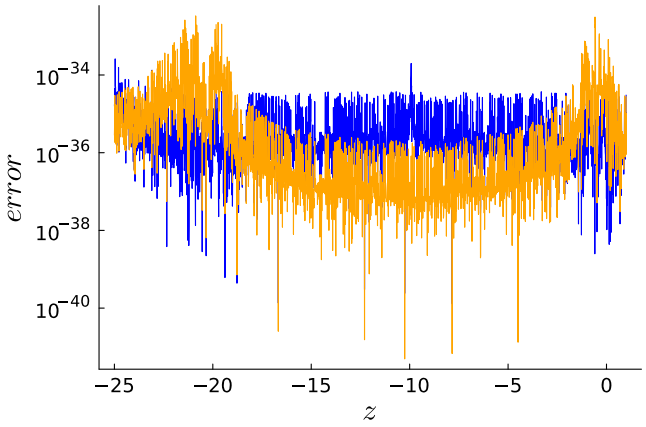

FIG. 3. The absolute (blue line) and relative error (orange line) of the numerical solution with $z_0 = 3 \times 10^8$, $\Delta = 0.01$, $\beta = 1$, $R_s = 10^5$. The absolute error is defined as $\epsilon_a = \frac{1}{4}\sum_i |\frac{\mathrm{d}N[f_i](z)}{\mathrm{d}z} - \mathcal{F}_{f_i}(N[f](z))|, f_i \in f = \{\zeta_1, \zeta_2, \xi, \psi\}$, where $N[f]$ represents the numerical solution and $\mathcal{F}_f(z)$ is given by the equation of motion (122). Similarly, the relative error is defined as $\epsilon_r = \frac{1}{4}\sum_i |\frac{\frac{\mathrm{d}N[f_i](z)}{z} - \mathcal{F}_{f_i}(N[f](z))}{\mathcal{F}_{f_i}(N[f](z)}|$.

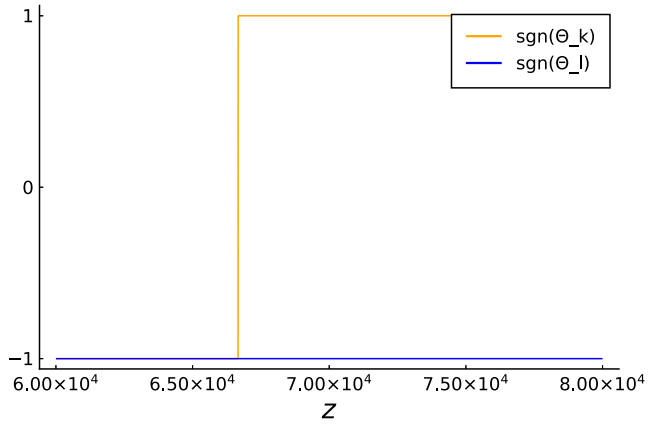

FIG. 4. Plots of $\mathrm{sgn}(\Theta_k)$ (orange) and $\mathrm{sgn}(\Theta_l)$ (blue) of the numerical solution with $z_0 = 3\times 10^8$, $\Delta = 0.01$, $\beta = 1$, $R_s = 10^5$. $\Theta_k = 0$ is at $z_H \simeq 6.67\times 10^4 \simeq \frac{2}{3}R_s$. The correction $|z_H - 2R_s/3| \sim 10^{-9}$.

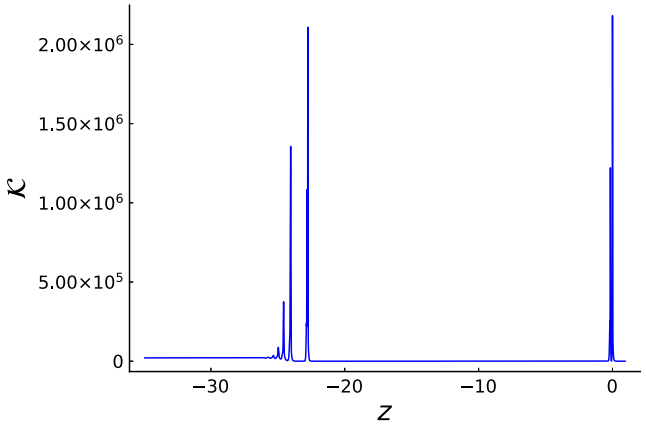

FIG. 5. Plot of Kretschmann invariant $\mathcal{K}$ of the numerical solutions with $z_0 = 3\times 10^8$, $\Delta = 0.01$, $R_s = 10^5$.

surface locals at $z \simeq z_H$ with negligible correction. The location of the marginal trapped surface is given by $\Theta_k = 0$ and $\Theta_l < 0$, where Θ_k and Θ_l are outward and inward null expansions (see Fig. 4). The marginal trapped surface corresponds to the killing horizon in the spacetime, although it is not the event horizon since the singularity is resolved.[5]

The Kretschmann invariant $\mathcal{K} = R^{\mu\nu\rho\sigma}R_{\mu\nu\rho\sigma}$ is bounded, as shown in FIG. 5. The black hole singularity at $z = 0$ is resolved. The spacetime geometries extend smoothly to $z < 0$. It demonstrates two groups of local maxima of $\mathcal{K}$ located, respectively, in the neighborhood N_0 of $z = 0$ and in a neighborhood $N_<$ of $z < 0$. We compute the maximal value of $\mathcal{K}$ in N_0 and $N_<$, respectively, denote them by $\mathcal{K}_{\mathrm{max},0}$ and $\mathcal{K}_{\mathrm{max},<}$, and test their dependence on Δ. The numerics demonstrate that both $\mathcal{K}_{\mathrm{max},0}$ and $\mathcal{K}_{\mathrm{max},<}$ are proportional to Δ^{-2} (see Fig. 6). If $\Delta \sim \ell_P^2$ relates to the minimal area gap in LQG, then the behavior of Kretschmann scalar $\mathcal{K}_{\mathrm{max},0}, \mathcal{K}_{\mathrm{max},<} \sim \Delta^{-2}$ indicates that the singularity resolution happens at the Planckian curvature. The distance $|z|$ between the locations of two maxima $\mathcal{K}_{\mathrm{max},0}$ and $\mathcal{K}_{\mathrm{max},<}$ relates to both Δ and R_s and behaves as $|z| \sim R_s^{1/3}\Delta^{1/3}$, see Fig. 7. Asymptotically for large negative z, $\mathcal{K}$ approaches to be z-independent constant, whose dependence on Δ is still $\sim\Delta^{-2}$. We come back to this asymptotic behavior shortly.

Figure 8 demonstrates $E^x, \log(E^\varphi), \zeta_1\sqrt{\Delta}, \zeta_2\sqrt{\Delta}$ of the numerical solution, when evolving smoothly across the Schwarzschild singularity at $z = 0$ and extending to $z < 0$. From Fig. 8(a), the evolution of E^x shows that the radial coordinate $r = \sqrt{E^x}$ is not a good coordinate anymore when extending the spacetime to $z < 0$, since $r = \sqrt{E^x}$ is not monotonic in the evolution. (t, x) are good coordinates for the extended spacetime due to the regularity of the metric components. As $z \to -\infty$, E^x, ζ_1, ζ_2 approach the constants while $E^\varphi \sim e^{-z/a_0 - a_1}$ with $a_0, a_1 > 0$. We denote by $E^x \sim r_0^2$ the constant as $z \to -\infty$. The solution indicates that the spacetime geometry approaches asymptotically the following metric as $z \to -\infty$

$$\mathrm{d}s^2 \sim -\mathrm{d}t^2 + r_0^{-2}e^{2(t-x)/a_0 - 2a_1}\mathrm{d}x^2 + r_0^2(\mathrm{d}\theta^2 + \sin^2\theta\mathrm{d}\varphi^2). \tag{130}$$

This metric is the $\mathrm{dS}_2 \times S^2$ geometry with $\mathrm{dS}_2 \times S^2$-radius a_0 and S^2-radius r_0. The geometry is also known as the Nariai geometry [73,74]. Here the existence of $\mathrm{dS}_2 \times S^2$ is a consequence of the covariant $\bar{\mu}$-scheme Hamiltonian, which comes from the higher derivative coupling in the mimetic gravity. Indeed both r_0 and a_0 depend on Δ. The dependence of r_0 and a_0 on Δ is analyzed numerically, and the results are shown in Fig. 9. The results indicate the following scaling properties of r_0 and a_0:

$$r_0, a_0 \propto \sqrt{\Delta}. \tag{131}$$

Both the sphere radius r_0 and the effective cosmological constant $1/a_0^2 \sim \Delta^{-1}$ relate to the quantum effect. In $\mathrm{dS}_2 \times S^2$, the Kretschmann invariant does not depend on z: $\mathcal{K}_{\mathrm{dS}_2\times S^2} = 4(a_0^{-4} + r_0^{-4}) \sim \Delta^{-2}$. This explains the asymptotically constant behavior of $\mathcal{K}$ as $z \to -\infty$ in Fig. 5. The ratio between $\mathcal{K}_{\mathrm{max},0}$ and $\mathcal{K}_{\mathrm{dS}_2\times S^2}$ is approximately 104.556. Compared to the result presented in [8], we obtain a similar scaling of the effective cosmological constant $1/\alpha_0^2$, but a different result for r_0. In our case, the minimum area of the asymptotically Nariai geometry given by the sphere radius r_0 is always larger than the minimum area gap Δ, so it is consistent, in contrast to the result

[5]Here we define the event horizon as the boundary of the past of the whole $\mathscr{I}^+$ instead the boundary of the past of the null part of $\mathscr{I}^+$, which can be seen from the spacetime diagram is shown in Fig. 10.

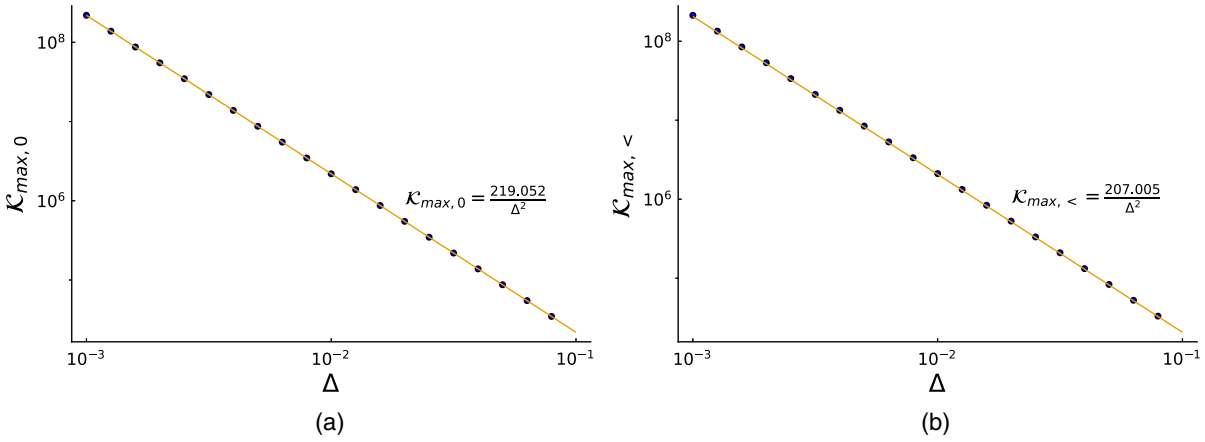

FIG. 6. (a) Δ versus the maximum $\mathcal{K}_{\max,0}$, for z inside the neighborhood N_0. (b) Δ versus the maximum of $\mathcal{K}_{\max,<}$, for z inside the neighborhood $N_<$.

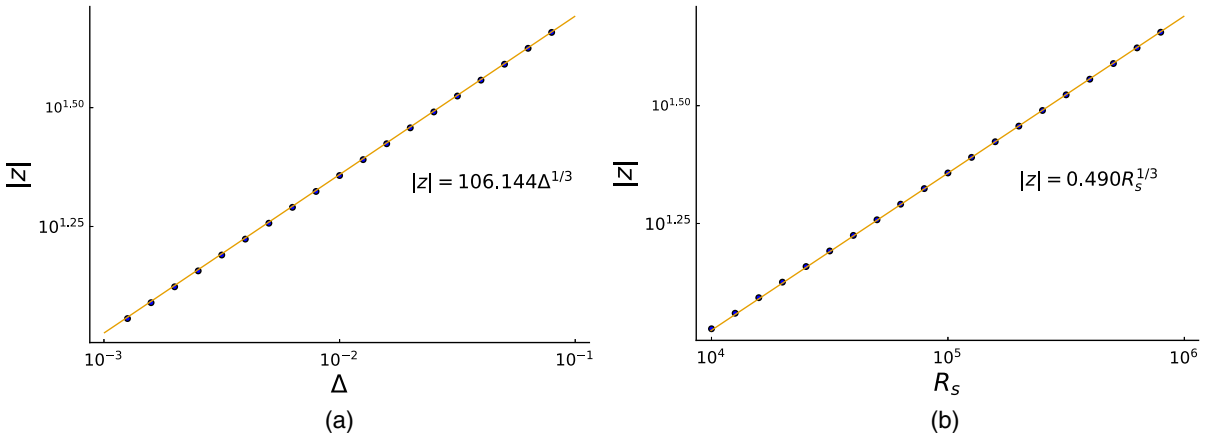

FIG. 7. The distance $|z|$ between the locations of two $\mathcal{K}$ maxima in N_0 and $N_<$ and the relations with Δ and R_s.

presented in [8]. A more detailed discussion of such a consistency check is given in Sec. VIII.

Recall that the 4D spacetime manifold is a product $\mathcal{M}_4 \simeq \mathcal{M}_2 \times S^2$, when we study the spherical symmetric gravity. If we suppress the S^2 factor and focus on the geometry on the 2D manifold $\mathcal{M}_2$, then the 2D spacetime $h_{ij}\mathrm{d}x^i\mathrm{d}x^j = -\mathrm{d}t^2 + \frac{(E^\varphi)^2}{E^x}\mathrm{d}x^2$ given by the solution leads to the conformal diagram as in Fig. 10. The maximal extension is given in Fig. 11 (see the Appendix for the conformal factor used for the diagram). The entire 2D spacetime is nonsingular, and has the complete null infinity $\mathscr{I}^+$. A part of $\mathscr{I}^+$ is spacelike as the null infinity of the asymptotic dS_2, while the other part of $\mathscr{I}^+$ is null as the null infinity of the asymptotic Schwarzschild geometry. The point in the conformal diagram where the spacelike and null parts of $\mathscr{I}^+$ meet is the timelike infinity i_+ for spacetime region outside the black hole, and it corresponds the spatial infinity i_0 for the asymptotic dS_2, although it is not the spatial infinity of the entire spacetime.

There is no event horizon due to the singularity resolution. $z \simeq z_H$ foliated by the marginal trapped surfaces is a killing horizon.[6] We have called the region inside the killing horizon the black hole interior.

Figure 10 is the conformal diagram for the 2D spacetime rather than the full 4D spacetime, because the four-dimensional $\mathrm{dS}_2 \times S^2$ metric dividing the conformal factor gives vanishing S^2 radius at $\mathscr{I}^+$. Note that this conformal diagram is the same as the one obtained in [24].

An interesting feature of the black hole solution is demonstrated by plotting the trajectory of the z evolution in the (ζ_1, ζ_2) space, shown in Fig. 12. The evolutions of ζ_1, ζ_2 are the keys of the $\bar{\mu}$-scheme dynamics, because they

[6]The killing vector has the norm $g_{\mu\nu}\xi^\mu\xi^\nu = -1 + e^{2\xi(z)}$. Comparing to the expansions $\Theta_k = (e^{-\xi(z)} - 1)\frac{\psi'(z)}{\sqrt{2}}$ and $\Theta_l = -(e^{-\xi(z)} + 1)\frac{\psi'(z)}{\sqrt{2}}$ shows that the killing vector is null when $\Theta_k = 0$ and $\Theta_l < 0$.

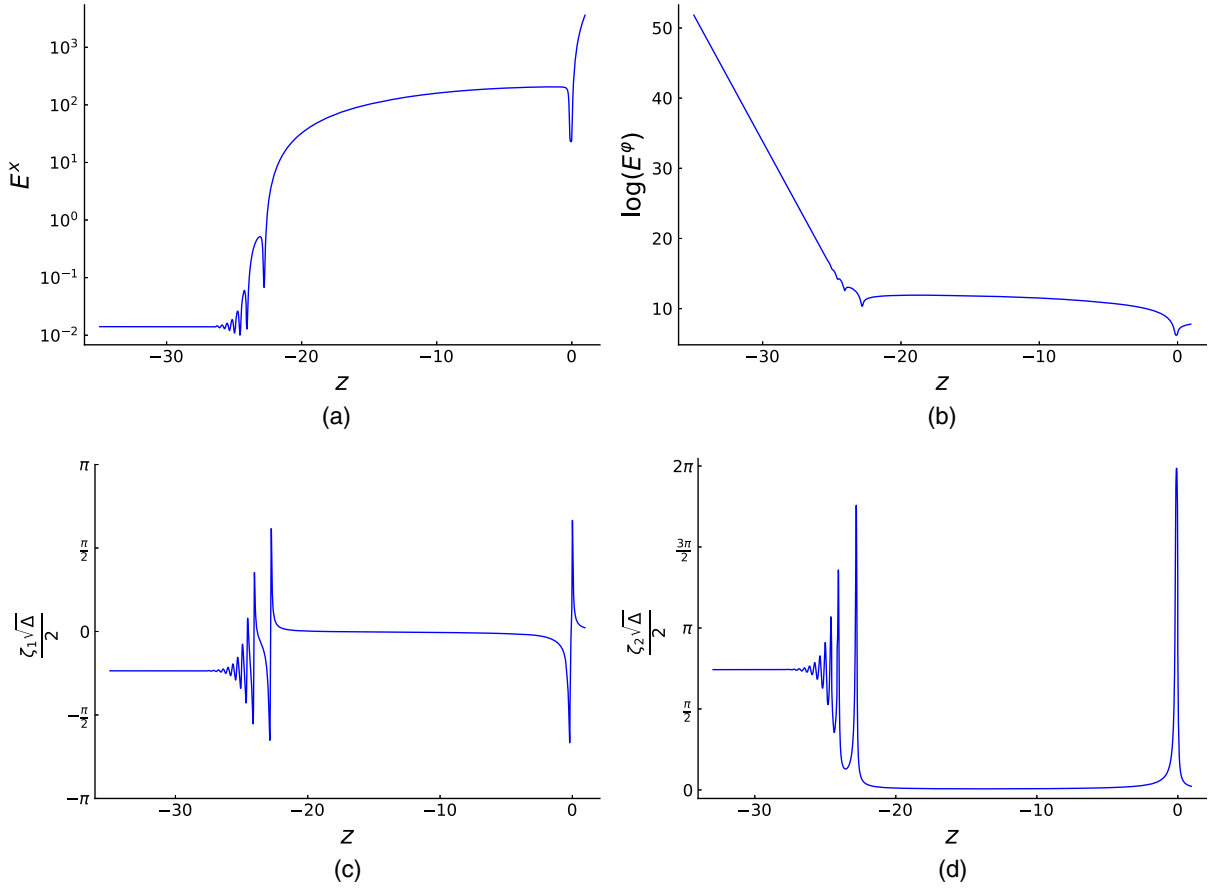

FIG. 8. Plots of $E^x = e^{2\psi}, \log(E^\varphi) = \psi + \xi, \zeta_1\sqrt{\Delta}, \zeta_2\sqrt{\Delta}$ of the numerical solutions in the regime $z < 1$ with $z_0 = 3 \times 10^8$, $\Delta = 0.01$, $R_s = 10^5$.

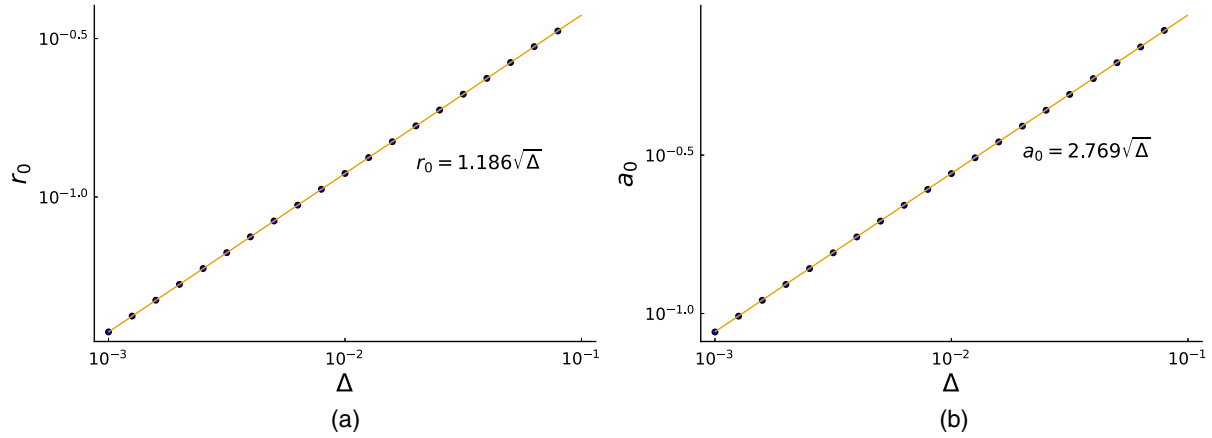

FIG. 9. The blue dots are the numerical values of r_0, a_0 from the solutions at different values of $\Delta \in [10^{-3}, 10^{-1}]$. The orange lines plot the best fit functions. Other parameters used in the numerics are $z_0 = 3 \times 10^8$, $R_s = 10^5$.

determines ψ, ξ thus the metric by (119) and (120). The z evolution begins with (0,0) in the (ζ_1, ζ_2) space and gives a spiral curve falling into the attractor. The covariant $\bar{\mu}$-scheme effective equations (123)–(126) have two types of sine/cosine functions of ζ_1 and ζ_2, respectively, so the trajectory in the (ζ_1, ζ_2) space is bounded. Moreover, viewing ζ_1, ζ_2 as the subsystem and ξ, ψ as the "environment," the coupling between ζ_1, ζ_2 and ξ, ψ leads to the "dissipation" causing the radius of the circular trajectory to shrink during the evolution thus resulting in the spiral

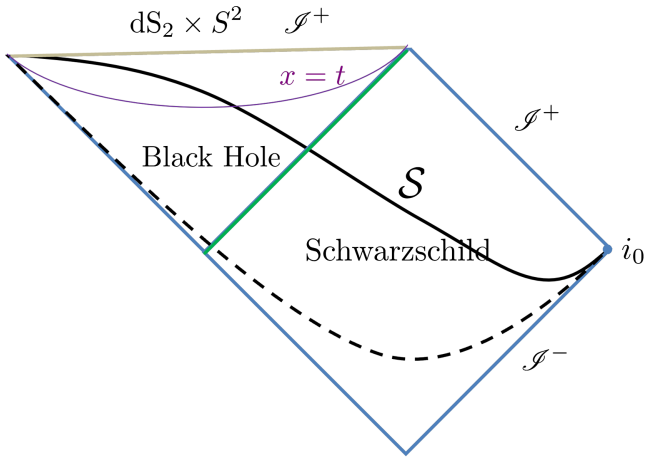

FIG. 10. The conformal diagram of the nonsingular black hole spacetime reduced to 2D covered by (t, x) coordinate. $\mathcal{S}$ (black curve) is a typical spatial slice with constant t. Dashed curves are another spatial slice in the far past. The green line illustrate the killing horizon. Near the future infinity, the 4D asymptotic geometry is $dS_2 \times S^2$ with Planckian radii.

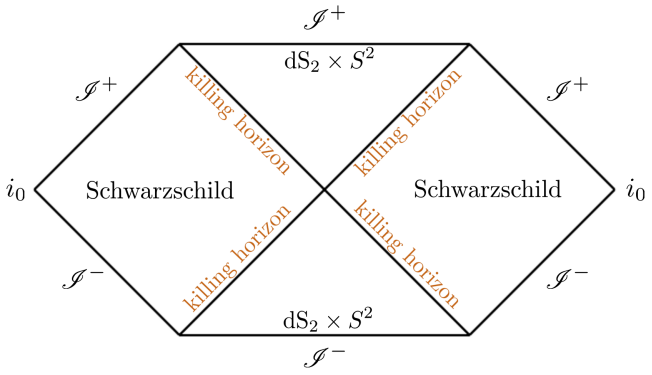

FIG. 11. The conformal diagram of the 2D maximal extension.

curve. The trajectory converges to the attractor that corresponds to the $dS_2 \times S^2$ geometry. This phenomena is common in the dissipative dynamical systems [75]. Figure 12 suggests that there should be an "basin of attraction" inside which any initial value of (ζ_1, ζ_2) evolves convergently to the $dS_2 \times S^2$ attractor.

B. Null expansion, stress-energy tensor, and quasinormal oscillation near $ds_2 \times s^2$

In the spherical symmetric spacetime (112), the outward and inward null geodesic congruences are generated by $k = \frac{1}{\sqrt{2}}(\partial_t + \frac{\sqrt{E^x}}{E^\varphi}\partial_x)$ and $l = \frac{1}{\sqrt{2}}(\partial_t - \frac{\sqrt{E^x}}{E^\varphi}\partial_x)$. Their expansions are given by

$$\Theta_k = \frac{1}{2}\tilde{h}^{\alpha\beta}\nabla_\alpha k_\beta = \frac{E^{x\prime}}{2\sqrt{2}\sqrt{E^x}E^\varphi} - \frac{E^{x\prime}}{2\sqrt{2}E^x} = (e^{-\xi} - 1)\frac{\psi'}{\sqrt{2}}, \tag{132}$$

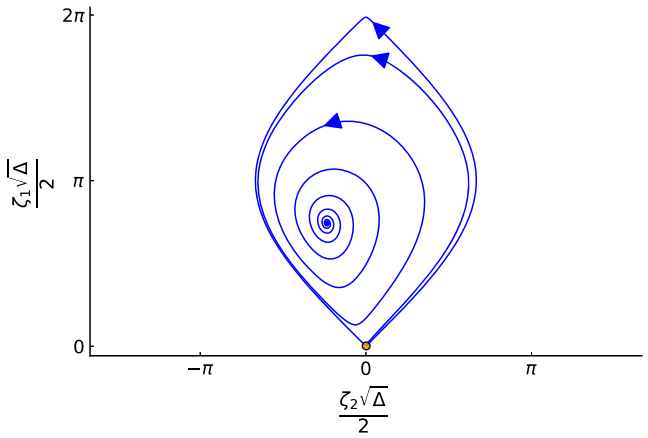

FIG. 12. This figure plots the trajectory of the z evolution in the (ζ_1, ζ_2) space. The arrow indicates the direction of the evolution from $z > 0$ to $z < 0$. The orange dot indicates the initial value of ζ_1, ζ_2 at z_0. The attractor is the $dS_2 \times S^2$ geometry.

$$\Theta_l = \frac{1}{2}\tilde{h}^{\alpha\beta}\nabla_\alpha l_\beta = -\frac{E^{x\prime}}{2\sqrt{2}\sqrt{E^x}E^\varphi} - \frac{E^{x\prime}}{2\sqrt{2}E^x} = (-e^{-\xi} - 1)\frac{\psi'}{\sqrt{2}}, \tag{133}$$

where $\tilde{h}_{\alpha\beta}$ is the induced metric on S^2. At the killing horizon $z \simeq \frac{2}{3}R_s$, Θ_k flips sign from positive to negative, while Θ_l keeps negative. For $z < \frac{2}{3}R_s$, Θ_k and Θ_l are of the same sign, although they can flips signs at the same time. In particular, when $z < 0$, we have that $e^{-\xi} \ll 1$ is negligible in Θ_k and Θ_l, so we have $\Theta_k \simeq \Theta_l \simeq -\psi'/\sqrt{2}$ in this regime (see Fig. 13 from the numerical solution discussed in Sec. VII A).

Θ_k, Θ_l are oscillatory for $z < 20$ [see Fig. 13(a)] and give many transition surfaces, at which both Θ_k, Θ_l change signs at the same time. Finally the expansions stabilize at $\Theta_k = \Theta_l = 0$ in the asymptotic $dS_2 \times S^2$ geometry, where $\psi' = 0$ thus the S^2 area is a constant instead of r^2 where r is the radius. The oscillation of Θ_k, Θ_l is purely a consequence of the oscillation of the S^2 area $E^x = e^{2\psi}$, since $\Theta_k \simeq \Theta_l \simeq -\psi'/\sqrt{2}$ in this regime.

Similar to the discussion of cosmology, we extract the energy momentum tensor $T'_{\mu\nu}$ by the Einstein equation $G_{\mu\nu} = T'_{\mu\nu}$. From the viewpoint of the effective dynamics of LQG, $T'_{\mu\nu}$ is the effective stress-energy tensor counting the quantum correction to the Einstein equation, while it is also the stress-energy tensor of the mimetic field from the mimetic-gravity point of view. In the (t, x, θ, φ) coordinate, $T'_{\mu\nu}$ depends only on four independent components T_{tt}, T_{tx}, T_{xx}, and $T_{\theta\theta}$

$$T'_{\mu\nu} = \begin{pmatrix} T_{tt} & T_{tx} & 0 & 0 \\ T_{tx} & T_{xx} & 0 & 0 \\ 0 & 0 & T_{\theta\theta} & 0 \\ 0 & 0 & 0 & T_{\theta\theta}\sin^2(\theta) \end{pmatrix}. \tag{134}$$

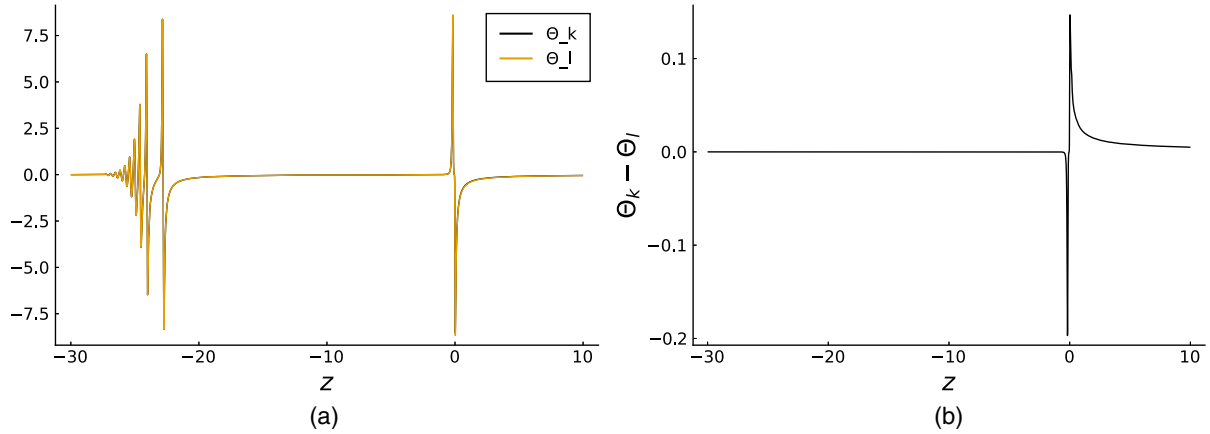

FIG. 13. (a) The plots of expansions Θ_k and Θ_l for $z \leq 10$. (b) The plots of the difference $\Theta_k - \Theta_l$.

The oscillation of the S^2 area relates to the oscillations of $T_{\theta\theta}$ and $T^{\mu\nu}\nabla_{\mu r}\nabla_{\nu r}$ (with $r = \sqrt{E^x}$), where $T_{\theta\theta}$ is the tension of the effective quantum matter (or equivalently, the mimetic field) wrapping on S^2, and $T^{\mu\nu}\nabla_{\mu r}\nabla_{\nu r}$ is the pressure normal to S^2. See Fig. 14(a) for the tension $T_{\theta\theta}$ and Fig. 14(b) for the pressure $T^{\mu\nu}\nabla_\mu r\nabla_\nu r$ (enlarged in the regime where $z < 20$ and the geometry is transiting to $dS_2 \times S^2$) from the numerical solution in Sec. VII A.

The effective energy density and the norm of energy flow $g^{\mu\nu}T_{t\mu}T_{t\nu}$ are plotted in Figs. 14(c) and 14(d). T_{tt} is always positive. $g^{\mu\nu}T_{t\mu}T_{t\nu}$ is positive in a small region near $z = 0$, where the dominant energy condition is violated, $g^{\mu\nu}T_{t\mu}T_{t\nu}$ is zero or negative elsewhere.

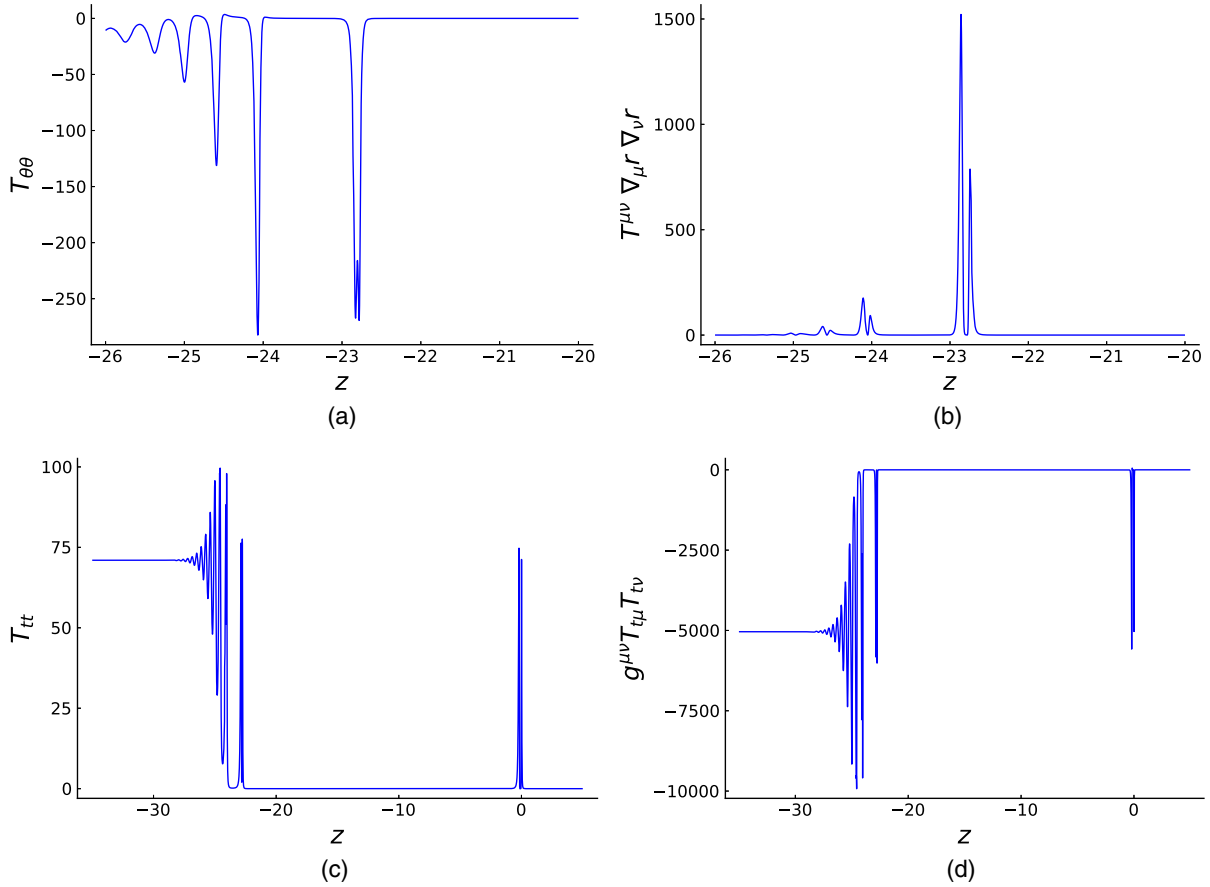

FIG. 14. (a) The plot of the effective tension on S^2. (b) The plot of the effective energy density. (c) The effective energy density. (d) The plot of the norm of the effective energy flow.

In order to clarify the oscillatory behavior of the geometry as approaching to the asymptotic $dS_2 \times S^2$, we perform the perturbations of the $dS_2 \times S^2$ geometry in the regime of large negative z:

$$\psi(z) = \log(r_0)[1 + p_1(z)],$$
$$\xi(z) = \left[-\frac{z}{a_0} - a_1 - \log(r_0)\right][1 + p_2(z)], \tag{135}$$

$$\zeta_1(z) = \mathring{\zeta}_1[1 + f_1(z)], \qquad \zeta_2(z) = \mathring{\zeta}_2[1 + f_2(z)], \tag{136}$$

where $\mathring{\zeta}_1$ and $\mathring{\zeta}_1$ are the asymptotical constant values of ζ_1 and ζ_2 as $z \to -\infty$ [see Figs. 8(c) and 8(d)]. The linearization of (123)–(126) and the expansion in e^{z/a_0} give

$$p_1'(z) = \frac{\mathring{\zeta}_1 f_1(z)\cos(\frac{\sqrt{\Delta}\mathring{\zeta}_1}{4}) + \mathring{\zeta}_2 f_2(z)\cos(\frac{\sqrt{\Delta}\mathring{\zeta}_2}{2})}{4\log(r_0)} + O(e^{z/a_0}), \tag{137}$$

$$p_2'(z) = \frac{a_0\mathring{\zeta}_2 f_2(z)\cos(\frac{\sqrt{\Delta}\mathring{\zeta}_2}{2}) - 4p_2(z)}{4(a_0 a1 + a_0\log(r_0) + z)} + O(e^{z/a_0}), \tag{138}$$

$$f_1'(z) = -\frac{f_1(z)\sin(\frac{\sqrt{\Delta}\mathring{\zeta}_2}{2})}{2\sqrt{\Delta}} - \frac{2f_1(z)\sin(\frac{\sqrt{\Delta}\mathring{\zeta}_1}{4})}{\sqrt{\Delta}} - \frac{1}{4}\mathring{\zeta}_2 f_2(z)\cos\left(\frac{\sqrt{\Delta}\mathring{\zeta}_2}{2}\right) - \frac{\mathring{\zeta}_2^2}{2\mathring{\zeta}_1} f_2(z)\cos\left(\frac{\sqrt{\Delta}\mathring{\zeta}_2}{2}\right) + O(e^{z/a_0}), \tag{139}$$

$$f_2'(z) = -\frac{\mathring{\zeta}_1^2 f_1(z)\cos(\frac{\sqrt{\Delta}\mathring{\zeta}_1}{4})}{4\mathring{\zeta}_2} - \frac{1}{2}\mathring{\zeta}_1 f_1(z)\cos\left(\frac{\sqrt{\Delta}\mathring{\zeta}_1}{4}\right) - \frac{2f_2(z)\sin(\frac{\sqrt{\Delta}\mathring{\zeta}_1}{4})}{\sqrt{\Delta}} - \frac{f_2(z)\sin(\frac{\sqrt{\Delta}\mathring{\zeta}_2}{2})}{2\sqrt{\Delta}} + \frac{4p_1(z)\log(r_0)}{\mathring{\zeta}_2 r_0^2} + O(e^{z/a_0}). \tag{140}$$

We evaluate $a_0, r_0, \mathring{\zeta}_1, \mathring{\zeta}_2$ at $z = z_f$ with a large negative z_f from the numerical solution (with $\Delta = 10^{-2}$ and $R_s = 10^5$) in Sec. VII A. The solution neglecting $O(e^{z/a_0})$ is obtained explicitly:

$$p_1(z) = (0.0738514c_1 - 0.232818c_2 + 0.835002c_3)e^{3.61642z} + e^{1.80821z}[(-0.0738514c_1 + 0.232818c_2 + 0.164998c_3)\cos(17.1418z) + (0.0866379c_1 + 0.24505c_2 - 0.193565c_3) \times \sin(17.1418z)], \tag{141}$$

$$p_2(z) = \frac{e^{1.80821z}}{(164.651 - 1.z)}[(0.0972387c_3 - 0.0435231c_1) \times \cos(17.1418z) + (0.00459104c_1 + 0.129943c_2 - 0.0102572c_3) \times \sin(17.1418z)], \tag{142}$$

$$f_1(z) = (0.164998c_1 - 0.52016c_2 + 1.86555c_3)e^{3.61642z} + e^{1.80821z}((0.835002c_1 + 0.52016c_2 - 1.86555c_3) \times \cos(17.1418z) + (0.0880803c_1 - 2.43812c_2 - 0.196788c_3) \times \sin(17.1418z)), \tag{143}$$

$$f_2(z) = e^{1.80821z}[c_2\cos(17.1418z) + (0.338666c_1 + 0.105485c_2 - 0.756645c_3) \times \sin(17.1418z)]. \tag{144}$$

c_1, c_2, c_3 are integration constants, and there is another integration constant c_4 vanishing due to the boundary condition $p_1, p_2, f_1, f_2 \to 0$ at $z = z_f$. The solution demonstrates the quasinormal oscillations of the perturbations and explains the behavior of the geometry when approaching to the $dS_2 \times S^2$ geometry. The frequency of the oscillation is $\omega = 17.1418$, while the amplitude of the oscillation is decaying exponentially as $z \to -\infty$ by the factor $e^{1.80821z} = e^{z/a_0}$.

VIII. ON THE CONSISTENCY AND UNIQUENESS OF COVARIANT $\bar{\mu}$ SCHEME

The covariant $\bar{\mu}$-scheme Hamiltonian (111) depends on the linear combinations of terms of the following $\bar{\mu}$-scheme holonomies:

$$h_x = \exp\left(\frac{i\beta\sqrt{\Delta}\sqrt{E^x}}{E^\varphi}2K_x\right),$$
$$h_\theta = h_\varphi = \exp\left(\frac{i\beta\sqrt{\Delta}}{\sqrt{E^x}}K_\varphi\right). \tag{145}$$

Here Δ is identified to the minimal nonzero eigenvalue in the LQG area spectrum. Recall the discussion in Sec. II that the $\bar{\mu}$-scheme polymerization in LQG uses the loop holonomies $h_\Delta(\square)$ around fundamental plaquettes with the fixed area that is set to Δ. There are two types of fundamental plaquettes $\square(\theta, \varphi)$ and $\square(x, \varphi)$, where $\square(\theta, \varphi)$ is in any 2-sphere with constant x and $\square(x, \varphi)$ is in the $x - \varphi$ cylinder at $\theta = \pi/2$. Their physical areas are

$$\mathrm{Ar}(\square(\theta, \varphi)) = 4\pi E^x \delta_\theta \delta_\varphi = \Delta,$$
$$\mathrm{Ar}(\square(x, \varphi)) = 2\pi E^\varphi \delta_x \delta_\varphi = \Delta, \tag{146}$$

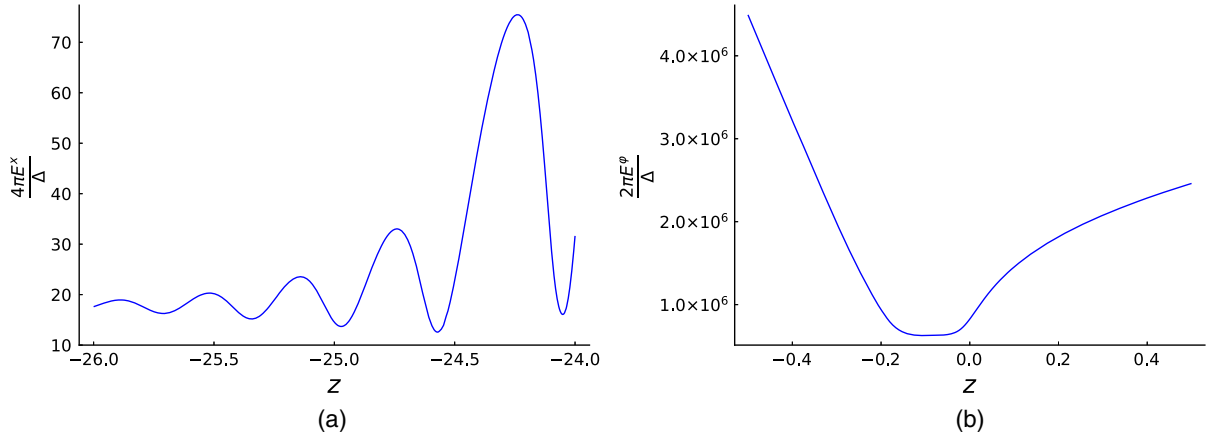

FIG. 15. The subfigures (a) and (b) plot, respectively, the regimes where E^x and E^φ reach their minima in the evolution. The parameters used in the figures are the same as in Fig. 8.

where $\delta_x, \delta_\theta, \delta_\varphi$ are coordinate lengths of the plaquette edges. The covariant $\bar{\mu}$-polymerization must respect these fundamental plaquettes. So $\delta_\theta\delta_\varphi < 1$, i.e. $4\pi E^x/\Delta > 1$, must hold in the entire evolution, such that there are always enough room on the 2-sphere to accommodate $\square(\theta,\varphi)$ with the area Δ. Indeed, this requirement is fulfilled by the black hole solution from the covariant $\bar{\mu}$-scheme dynamics. Figure 15 shows that we have $\delta_\theta\delta_\varphi < 1/10 < 1$ and $\delta_x\delta_\varphi \lesssim 10^{-5} < 1$. Therefore the covariant $\bar{\mu}$-scheme dynamics of the nonsingular black hole is self-consistent.

Recall that there is freedom in choosing the parameters $a, c, h, \alpha_1, \alpha_2$ in the covariant $\bar{\mu}$-scheme Hamiltonian, and the cosmological effective dynamics provides a restriction to the parameters due to the consistency condition (95). The above discussion is based on the choice (96) satisfying the consistency condition. But there exists other choices classified below (101), which are allowed by the cosmological effective dynamics. Let us discuss the implications from these choices to the spherical symmetric effective Hamiltonian:

(1) $c = h$ and $\beta = 2a_2/h$ gives the covariant $\bar{\mu}$-scheme Hamiltonian with

$$\mathcal{C}_\Delta = \frac{\sqrt{E^x}E^\varphi}{\Delta G}\left[\frac{3a^2\sin^2\left(\frac{4\alpha_1\sqrt{\Delta}\sqrt{E^x}K_x}{3aE^\varphi} - \frac{2\alpha_1\sqrt{\Delta}K_\varphi}{3a\sqrt{E^x}}\right)}{8\alpha_1^2} - \frac{3\sin^2\left(\frac{2\beta\sqrt{\Delta}\sqrt{E^x}K_x}{3E^\varphi} + \frac{2\beta\sqrt{\Delta}K_\varphi}{3\sqrt{E^x}}\right)}{2\beta^2}\right] + \frac{1}{4G\sqrt{E^x}}\left(-\frac{2E^xE^{x\prime}E^{\varphi\prime}}{E^{\varphi 2}} + \frac{4E^xE^{x\prime\prime} + E^{x\prime 2}}{2E^\varphi} - 2E^\varphi\right). \tag{147}$$

The $\bar{\mu}$-scheme holonomies in this Hamiltonian contain

$$h_x = \exp\left(\frac{\rho}{2}\frac{i\beta\sqrt{\Delta}\sqrt{E^x}}{E^\varphi}2K_x\right),$$
$$h_\theta = h_\varphi = \exp\left(\rho\frac{i\beta\sqrt{\Delta}}{\sqrt{E^x}}K_\varphi\right), \qquad \rho = \frac{4}{3}. \tag{148}$$

These holonomies are along the edges with the fixed geometrical length $\rho\sqrt{\Delta} \equiv \sqrt{\Delta_0}$. Given that the cosmological effective dynamics has the $\bar{\mu}$-scheme holonomy $\exp(i\beta\sqrt{\Delta}b)$, $\Delta \neq \Delta_0$ in this scheme implies that the black hole and cosmology corresponds to the $\bar{\mu}$-scheme holonomies with different lengths. Then there is ambiguity about whether Δ or Δ_0 should be identified to the minimal area gap in LQG. Therefore, although this choice of parameter has no problem from the mimetic-gravity point of view, the inconsistency of $\bar{\mu}$-scheme holonomies suggests to exclude this choice from the LQG point of view.

(2) $c = -h/2$ and $\beta = 2\alpha_1/a$ gives the Hamiltonian with

$$\mathcal{C}_\Delta = \frac{\sqrt{E^x}E^\varphi}{\Delta G}\left[\frac{3h^2\sin^2\left(\frac{8\alpha_2\sqrt{\Delta}\sqrt{E^x}K_x}{3E^\varphi h}-\frac{4\alpha_2\sqrt{\Delta}K_\varphi}{3\sqrt{E^x}h}\right)}{32\alpha_2^2}-\frac{3\sin^2\left(\frac{2\beta\sqrt{\Delta}\sqrt{E^x}K_x}{3E^\varphi}+\frac{2\beta\sqrt{\Delta}K_\varphi}{3\sqrt{E^x}}\right)}{2\beta^2}\right] + \frac{1}{4G\sqrt{E^x}}\left(-\frac{2E^xE^{x\prime}E^{\varphi\prime}}{E^{\varphi 2}}+\frac{4E^xE^{x\prime\prime}+E^{x\prime 2}}{2E^\varphi}-2E^\varphi\right). \tag{149}$$

This Hamiltonian becomes the same as (147) by $h \to a$ and $\alpha_2 \to \alpha_1/2$. This choice of parameters has the same problem as the above, and thus it should be exclude by the consistency in LQG.

(3) For the choice $h = \frac{c(\alpha_1 c - 2\alpha_2 a)}{\alpha_2 a + \alpha_1 c}$ and $\beta = \frac{8\alpha_2\alpha_1}{\alpha_2 a - \alpha_1 c}$, it is convenient to introduce $m := \frac{\alpha_2}{\beta c}$. The Hamiltonian has

$$\mathcal{C}_\Delta = \frac{3\sqrt{E^x}E^\varphi}{8\beta^2\Delta G m(m+1)}\left[(1+2m)^2\sin^2\left(\frac{4(m+1)\beta\sqrt{\Delta}\sqrt{E^x}K_x}{3(2m+1)E^\varphi}+\frac{(4m+1)\beta\sqrt{\Delta}K_\varphi}{3(2m+1)\sqrt{E^x}}\right) -\sin^2\left(\frac{4(m+1)\beta\sqrt{\Delta}\sqrt{E^x}K_x}{3E^\varphi}+\frac{(1-2m)\beta\sqrt{\Delta}K_\varphi}{3\sqrt{E^x}}\right)\right] + \frac{1}{4G\sqrt{E^x}}\left(-\frac{2E^xE^{x\prime}E^{\varphi\prime}}{E^{\varphi 2}}+\frac{4E^xE^{x\prime\prime}+E^{x\prime 2}}{2E^\varphi}-2E^\varphi\right). \tag{150}$$

This choice includes (96) as a special case equivalent to $m = 1/2$. this special case results in the Hamiltonian (111) with the $\bar{\mu}$-scheme holonomies (145), whose length is the same as the $\bar{\mu}$-scheme holonomy in cosmology. So $m = 1/2$ does not have the above problem of inconsistency. Requiring (150) to only depend on the same holonomies as (145) constrains

$$\left(\frac{4(m+1)}{3}, \quad \frac{2}{3}(1-2m), \quad \frac{4(m+1)}{6m+3}, \quad \frac{2(4m+1)}{6m+3}\right) \in \mathbb{Z}^4. \tag{151}$$

If we define $n = \frac{4(m+1)}{3}$ and $k = \frac{4(m+1)}{6m+3}$, then (151) equals $(n, n-2, k, 2k)$ and thus implies both $n, k \in \mathbb{Z}$. By the definition of n, k, they are constrained by $\frac{2}{3}(k+n) = kn$ or $\frac{1}{n}+\frac{1}{k} = \frac{3}{2}$ if $n, k \neq 0$. It is only possible if $|n| \leq 2$ and $|k| \leq 2$. Indeed, we check that there are only three possibilities $n = 0, 1, 2$, which give

$$m = -1, \quad -1/4, \quad 1/2. \tag{152}$$

$m = -1$ is ruled out since it causes $\mathcal{C}_\Delta$ to diverge. $m = -1/4$ and $m = 1/2$ gives exactly the same $\mathcal{C}_\Delta$ as (111).

(4) The choice $h = \frac{c(\alpha_1 c + 2\alpha_2 a)}{-\alpha_2 a + \alpha_1 c}$ and $\beta = \frac{8\alpha_2\alpha_1}{-\alpha_2 a - \alpha_1 c}$ gives the same Hamiltonian as (150), so the discussion and result are the same as the above case.

In summary, among the Hamiltonians with $\mathcal{C}_\Delta$ in (80) derived from the mimetic gravity Lagrangian, $\mathcal{C}_\Delta$ in (111) stands out uniquely by requiring (1) the consistency condition (95) in cosmology, and (2) the consistency between the lengths of the $\bar{\mu}$-scheme holonomies in black hole and cosmology.

IX. CONCLUSION AND OUTLOOK

In this work, we propose the covariant $\bar{\mu}$-scheme effective dynamics of the spherical symmetric LQG. This effective dynamics can be derived from the covariant mimetic gravity Lagrangian in 4D, with the prescribed higher derivative couplings. The effective theory contains the LQC effective dynamics as a subsection. The theory gives the nonsingular black hole solution, which resolves the singularity in the Schwarzschild spacetime. The nonsingular black hole spacetime has the complete $\mathscr{I}^+$. In the interior of the black hole, the spacetime evolves to $\mathrm{dS}_2 \times S^2$ geometry as the asymptotic final state. The covariant mimetic gravity Lagrangian allows us to formulate the effective dynamics beyond the $3+1$ canonical formulation. In particular, it is useful to formulate the effective dynamics in the light cone gauge.

Compared to the previous work, we obtain a similar effective stationary spacetime as in [24]. However, a covariant Lagrangian is missing for the model proposed in [24], whereas in this work we find the underlying covariant mimetic gravity Lagrangian in 4D. The effective spacetime is different from the models presented in [25,26,76–78]. One of the most important differences is that we explicitly consider the holonomy (or polymerization) of K_x, while the models presented in [25,76,77] only consider the effect of K_ϕ. The model presented in [25] also has an underlying covariant mimetic Lagrangian and it admits a polymerized LTB condition, as pointed out

in [79,80]. However, in such models it seems that shell-crossing singularities will naturally appear [81], which can be understood from the point of view of limiting curvature, since in this case only one of the extrinsic curvatures K_ϕ is regularized. As a result, it seems that our approach will be free of shell-crossing singularities if we regularize both extrinsic curvatures, which we leave for a future study. We also note that [76–78] requires a closure of the hypersurface deformation algebra to ensure general covariance. In contrast, our Hamiltonian is obviously covariant, since it is formulated in reduced phase space and in terms of the Dirac observables.

As the applications of the covariant $\bar{\mu}$-scheme effective dynamics to the spherical symmetric LQG, the solutions of black hole and cosmology has more symmetries than only the spherical symmetry. The additional symmetries are used for simplifying the PDEs to ODEs. However, more interesting situations with richer dynamical properties often need to relax the additional symmetry and solve the full PDEs. One interesting dynamical situations is the gravitational collapse with massive or null matter (see [27,28,82] for some recent progress on the effective dynamics of gravitational collapse). The null shell collapse can be considered for the Callan-Giddings-Harvey-Strominger model [83] with mimetic extension, and understanding the full dynamics on the 2D spacetime requires us to solve the full PDEs. Another interesting situation is to include the backreaction of the Hawking radiation, which should result in the dynamical black hole solution. The black hole solution in this work does not have the white-hole type marginal antitrap surface, but it might be the consequence from the additional killing symmetry $\partial_t + \partial_x$. Treating the full PDEs should give the more interesting dynamical black hole solutions and provide different scenarios of the black hole final states.

ACKNOWLEDGMENTS

M. H. acknowledges Abhay Ashtekar for many enlightening discussions and his encouragement. In particularly, this work receives valuable contributions from Abhay Ashtekar on the covariance, the foliation and geometry of the nonsingular black hole, the null expansion, and the physical interpretation. The authors also acknowledges Eugenio Bianchi, Kristina Giesel, Lingzhen Guo, and Stefan Weigl for helpful discussions on aspects of Hamiltonian dynamics. M. H. receives support from the National Science Foundation through Grants No. PHY-1912278 and No. PHY-2207763, and the sponsorship provided by the Alexander von Humboldt Foundation during his visit at FAU Erlangen-Nürnberg. In addition, M. H. acknowledges IQG at FAU Erlangen-Nürnberg, IGC at Penn State University, Perimeter Institute for Theoretical Institute, and University of Western Ontario for the hospitality during his visits.

APPENDIX: CONFORMAL DIAGRAM AND MAXIMAL EXTENSION

The 2D metric is given by

$$h_{ij}\mathrm{d}x^i\mathrm{d}x^j = -\mathrm{d}t^2 + \frac{E^\varphi(z)^2}{E^x(z)}\mathrm{d}x^2, \qquad z = x - t. \tag{A1}$$

We introduce the new coordinate τ given by

$$\tau = t - \int_{z_0}^{z} dz' \frac{E^\varphi(z')^2}{E^\varphi(z')^2 - E^x(z')}. \tag{A2}$$

The 2D metric is expressed as below in the (τ, z) coordinate:

$$h_{ij}\mathrm{d}x^i\mathrm{d}x^j = -\frac{E^x - (E^\varphi)^2}{E^x}\mathrm{d}\tau^2 + \frac{(E^\varphi)^2}{E^x - (E^\varphi)^2}\mathrm{d}z^2. \tag{A3}$$

The coordinate transformation is singular at the killing horizon where $E^x = (E^\varphi)^2$.

We define two null coordinates

$$\begin{aligned} u &= \int_{z_0}^{z} dz' \frac{E^\varphi(z')\sqrt{E^x(z')}}{E^\varphi(z')^2 - E^x(z')} + \tau, \\ v &= \int_{z_0}^{z} dz' \frac{E^\varphi(z')\sqrt{E^x(z')}}{E^\varphi(z')^2 - E^x(z')} - \tau \end{aligned} \tag{A4}$$

and their rescaling

$$U = e^{A_0 - \frac{u}{2B_0}}, \qquad V = \mathrm{sgn}((E^\varphi)^2 - E^x)e^{A_0 - \frac{v}{2B_0}}, \tag{A5}$$

where $B_0 = |\frac{E^\varphi\sqrt{E^x}}{2E^\varphi E^{\varphi\prime} - E^{x\prime}}|_{(E^\varphi)^2 - E^x = 0}$. For a sufficiently large black hole, the value of B_0 is well approximated by the Schwarzschild one, which is $B_0 = R_s := \sqrt{E^x}|_{(E^\varphi)^2 - E^x = 0}$. We chose A_0 such that when $z \to \infty$ we have $UV = 1$. When z_0 is sufficiently large, A_0 is approximately given by the Schwarzschild one which reads

$$A_0 = \left(\frac{E^x}{2(E^\varphi)^2} + \frac{1}{2}\log\left|\frac{(E^\varphi)^2 - E^x}{(E^\varphi)^2}\right|\right)\Bigg|_{z=z_0}. \tag{A6}$$

$UV = 0$ indicates the location of the horizon. Using U and V we define

$$T = \frac{1}{2}(U + V), \qquad X = \frac{1}{2}(U - V) \tag{A7}$$

Here z is a function of UV thus a function of $T^2 - X^2$, and τ is a function of T/X. As a result, we can define the extension $(T, X) \to (-T, -X)$. With the Schwarzschild geometry, we recover the Kruskal-Szekeres coordinates

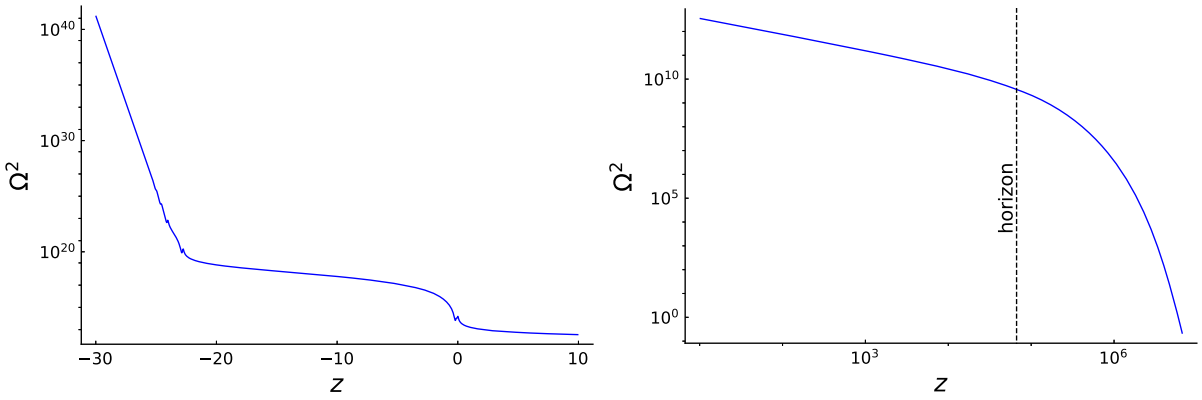

FIG. 16. Log-log plot of the conformal factor Ω^2 as a function of z.

$$T = e^{\frac{r}{2R_s}} \cosh\left(\frac{\tau}{2R_s}\right)\sqrt{1-\frac{r}{R_s}},$$
$$X = e^{\frac{r}{2R_s}} \sinh\left(\frac{\tau}{2R_s}\right)\sqrt{1-\frac{r}{R_s}} \tag{A8}$$

for z inside the horizon and

$$T = e^{\frac{r}{2R_s}} \sinh\left(\frac{\tau}{2R_s}\right)\sqrt{\frac{r}{R_s}-1},$$
$$X = e^{\frac{r}{2R_s}} \cosh\left(\frac{\tau}{2R_s}\right)\sqrt{\frac{r}{R_s}-1} \tag{A9}$$

for z outside the horizon.

The 2D metric is conformally flat

$$h_{ij}\mathrm{d}x^i\mathrm{d}x^j = \Omega^2(-dT^2 + dX^2) \tag{A10}$$

with the conformal factor as a function of z only

$$\Omega^2 = \mathrm{sgn}((E^\varphi)^2 - E^x)e^{-2A_0+\frac{u+v}{2R_s}}\frac{E^x}{R_s[(E^\varphi)^2 - E^x]} \tag{A11}$$

Ω^2 of the nonsingular black hole solution discussed in Sec. VII is plotted in Fig. 16. The right panel in Fig. 16 shows that Ω^2 is continuous at the horizon, while the left panel shows the exponential growth of Ω^2 as $z \to -\infty$.

We make the conformal compactification of the 2D spacetime by introducing

$$\tilde{U} = \arctan(U), \qquad \tilde{V} = \arctan(V), \tag{A12}$$

$$2\tilde{T} = \tilde{U} + \tilde{V}, \qquad 2\tilde{X} = \tilde{U} - \tilde{V}, \tag{A13}$$

where $\tilde{U}, \tilde{V} \in [-\pi/2, \pi/2]$. The metric is given by

$$h_{ij}\mathrm{d}x^i\mathrm{d}x^j = \tilde{\Omega}^2(-d\tilde{T}^2 + d\tilde{X}^2) \tag{A14}$$

with

$$\tilde{\Omega}^2 = \frac{\Omega^2}{\cos(\tilde{U})^2\cos(\tilde{V})^2}, \tag{A15}$$

where the factor $[\cos(\tilde{U})\cos(\tilde{V})]^{-1}$ comes from conformal compactification of flat spacetime. The conformal diagram is shown in Fig. 17.

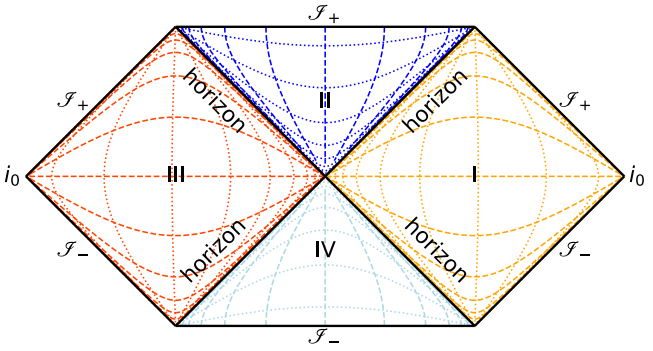

FIG. 17. The conformal diagram of the 2D spacetime from the nonsingular black hole solution. The dashed lines are the τ, z coordinate lines, where constant z lines are timelike outside (spacelike inside) the killing horizon.

[1] M. Bojowald, Absence of singularity in loop quantum cosmology, Phys. Rev. Lett. **86**, 5227 (2001).

[2] A. Ashtekar, T. Pawlowski, and P. Singh, Quantum nature of the big bang: Improved dynamics, Phys. Rev. D **74**, 084003 (2006).

[3] I. Agullo and P. Singh, Loop quantum cosmology, in *Loop Quantum Gravity: The First 30 Years*, edited by A. Ashtekar and J. Pullin (World Scientific, Singapore, 2017), pp. 183–240.

[4] M. Bojowald, Effective field theory of loop quantum cosmology, Universe **5**, 44 (2019).

[5] A. Ashtekar, Black hole evaporation: A perspective from loop quantum gravity, Universe **6**, 21 (2020).

[6] A. Ashtekar and M. Bojowald, Quantum geometry and the Schwarzschild singularity, Classical Quantum Gravity **23**, 391 (2006).

[7] L. Modesto, Loop quantum black hole, Classical Quantum Gravity **23**, 5587 (2006).

[8] C. G. Boehmer and K. Vandersloot, Loop quantum dynamics of the Schwarzschild interior, Phys. Rev. D **76**, 104030 (2007).

[9] N. Dadhich, A. Joe, and P. Singh, Emergence of the product of constant curvature spaces in loop quantum cosmology, Classical Quantum Gravity **32**, 185006 (2015).

[10] A. Ashtekar, F. Pretorius, and F. M. Ramazanoglu, Evaporation of 2-dimensional black holes, Phys. Rev. D **83**, 044040 (2011).

[11] D.-W. Chiou, W.-T. Ni, and A. Tang, Loop quantization of spherically symmetric midisuperspaces and loop quantum geometry of the maximally extended Schwarzschild spacetime, arXiv:1212.1265.

[12] R. Gambini, J. Olmedo, and J. Pullin, Quantum black holes in loop quantum gravity, Classical Quantum Gravity **31**, 095009 (2014).

[13] E. Bianchi, M. Christodoulou, F. D'Ambrosio, H. M. Haggard, and C. Rovelli, White holes as remnants: A surprising scenario for the end of a black hole, Classical Quantum Gravity **35**, 225003 (2018).

[14] F. D'Ambrosio, M. Christodoulou, P. Martin-Dussaud, C. Rovelli, and F. Soltani, The end of a black hole's evaporation—part I, Phys. Rev. D **103**, 106014 (2021).

[15] J. Brunnemann and T. Thiemann, On (cosmological) singularity avoidance in loop quantum gravity, Classical Quantum Gravity **23**, 1395 (2006).

[16] V. Husain and O. Winkler, Quantum resolution of black hole singularities, Classical Quantum Gravity **22**, L127 (2005).

[17] V. Husain and O. Winkler, Quantum black holes from null expansion operators, Classical Quantum Gravity **22**, L135 (2005).

[18] J. Olmedo, S. Saini, and P. Singh, From black holes to white holes: A quantum gravitational, symmetric bounce, Classical Quantum Gravity **34**, 225011 (2017).

[19] A. Ashtekar, J. Olmedo, and P. Singh, Quantum extension of the Kruskal spacetime, Phys. Rev. D **98**, 126003 (2018).

[20] M. Bojowald, S. Brahma, and D.-h. Yeom, Effective line elements and black-hole models in canonical loop quantum gravity, Phys. Rev. D **98**, 046015 (2018).

[21] N. Bodendorfer, F. M. Mele, and J. Münch, Effective quantum extended spacetime of polymer Schwarzschild black hole, Classical Quantum Gravity **36**, 195015 (2019).

[22] E. Alesci, S. Bahrami, and D. Pranzetti, Quantum gravity predictions for black hole interior geometry, Phys. Lett. B **797**, 134908 (2019).

[23] M. Assanioussi, A. Dapor, and K. Liegener, Perspectives on the dynamics in a loop quantum gravity effective description of black hole interiors, Phys. Rev. D **101**, 026002 (2020).

[24] M. Han and H. Liu, Improved effective dynamics of loop-quantum-gravity black hole and Nariai limit, Classical Quantum Gravity **39**, 035011 (2022).

[25] J. G. Kelly, R. Santacruz, and E. Wilson-Ewing, Black hole collapse and bounce in effective loop quantum gravity, Classical Quantum Gravity **38**, 04LT01 (2021).

[26] R. Gambini, J. Olmedo, and J. Pullin, Spherically symmetric loop quantum gravity: Analysis of improved dynamics, Classical Quantum Gravity **37**, 205012 (2020).

[27] K. Giesel, B.-F. Li, and P. Singh, Non-singular quantum gravitational dynamics of an LTB dust shell model: The role of quantization prescriptions, Phys. Rev. D **104**, 106017 (2021).

[28] J. Lewandowski, Y. Ma, J. Yang, and C. Zhang, Quantum Oppenheimer-Snyder and Swiss Cheese models, Phys. Rev. Lett. **130**, 101501 (2023).

[29] T. Clifton, P. G. Ferreira, A. Padilla, and C. Skordis, Modified gravity and cosmology, Phys. Rep. **513**, 1 (2012).

[30] A. H. Chamseddine and V. Mukhanov, Mimetic dark matter, J. High Energy Phys. 11 (2013) 135.

[31] L. Sebastiani, S. Vagnozzi, and R. Myrzakulov, Mimetic gravity: A review of recent developments and applications to cosmology and astrophysics, Adv. High Energy Phys. **2017**, 3156915 (2017).

[32] S. Nojiri and S. D. Odintsov, Mimetic $F(R)$ gravity: Inflation, dark energy and bounce, Mod. Phys. Lett. A **29**, 1450211(E) (2014).

[33] S. Nojiri, S. D. Odintsov, and V. K. Oikonomou, Unimodular-mimetic cosmology, Classical Quantum Gravity **33**, 125017 (2016).

[34] S. Nojiri, S. D. Odintsov, and V. K. Oikonomou, Ghost-free $F(R)$ gravity with Lagrange multiplier constraint, Phys. Lett. B **775**, 44 (2017).

[35] S. Nojiri, S. D. Odintsov, and V. K. Oikonomou, Ghost-free Gauss-Bonnet theories of gravity, Phys. Rev. D **99**, 044050 (2019).

[36] J. Ben Achour, F. Lamy, H. Liu, and K. Noui, Polymer Schwarzschild black hole: An effective metric, Europhys. Lett. **123**, 20006 (2018).

[37] D. Langlois, H. Liu, K. Noui, and E. Wilson-Ewing, Effective loop quantum cosmology as a higher-derivative scalar-tensor theory, Classical Quantum Gravity **34**, 225004 (2017).

[38] J. Ben Achour, F. Lamy, H. Liu, and K. Noui, Non-singular black holes and the limiting curvature mechanism: A Hamiltonian perspective, J. Cosmol. Astropart. Phys. 05 (2018) 072.

[39] N. Bodendorfer, A. Schäfer, and J. Schliemann, Canonical structure of general relativity with a limiting curvature and its relation to loop quantum gravity, Phys. Rev. D **97**, 084057 (2018).

[40] A. H. Chamseddine and V. Mukhanov, Nonsingular black hole, Eur. Phys. J. C **77**, 183 (2017).

[41] V. P. Frolov and A. Zelnikov, Spherically symmetric black holes in the limiting curvature theory of gravity, Phys. Rev. D **105**, 024041 (2022).
[42] M. Bojowald, Comment on "Towards a quantum notion of covariance in spherically symmetric loop quantum gravity", Phys. Rev. D **105**, 108901 (2022).
[43] R. Gambini, J. Olmedo, and J. Pullin, Towards a quantum notion of covariance in spherically symmetric loop quantum gravity, Phys. Rev. D **105**, 026017 (2022).
[44] M. Bojowald, Black-hole models in loop quantum gravity, Universe **6**, 125 (2020).
[45] M. Bojowald, S. Brahma, and J. D. Reyes, Covariance in models of loop quantum gravity: Spherical symmetry, Phys. Rev. D **92**, 045043 (2015).
[46] R. Tibrewala, Inhomogeneities, loop quantum gravity corrections, constraint algebra and general covariance, Classical Quantum Gravity **31**, 055010 (2014).
[47] A. H. Chamseddine and V. Mukhanov, Resolving cosmological singularities, J. Cosmol. Astropart. Phys. 03 (2017) 009.
[48] J. de Haro, L. Aresté Saló, and E. Elizalde, Cosmological perturbations in a class of fully covariant modified theories: Application to models with the same background as standard LQC, Eur. Phys. J. C **78**, 712 (2018).
[49] N. Bodendorfer, F. M. Mele, and J. Münch, Is limiting curvature mimetic gravity an effective polymer quantum gravity?, Classical Quantum Gravity **35**, 225001 (2018).
[50] G. J. Olmo and P. Singh, Effective action for loop quantum cosmology a la Palatini, J. Cosmol. Astropart. Phys. 01 (2009) 030.
[51] D. Langlois and K. Noui, Hamiltonian analysis of higher derivative scalar-tensor theories, J. Cosmol. Astropart. Phys. 07 (2016) 016.
[52] J. Ben Achour, M. Crisostomi, K. Koyama, D. Langlois, K. Noui, and G. Tasinato, Degenerate higher order scalar-tensor theories beyond Horndeski up to cubic order, J. High Energy Phys. 12 (2016) 100.
[53] D. Langlois, M. Mancarella, K. Noui, and F. Vernizzi, Mimetic gravity as DHOST theories, J. Cosmol. Astropart. Phys. 02 (2019) 036.
[54] M. de Cesare and V. Husain, Physical Hamiltonian for mimetic gravity, Phys. Rev. D **102**, 104052 (2020).
[55] Martin Bojowald (private communication).
[56] M. Bojowald and E. I. Duque, Inequivalence of mimetic gravity with models of loop quantum gravity, arXiv: 2401.15040.
[57] M. Bojowald and R. Swiderski, Spherically symmetric quantum geometry: Hamiltonian constraint, Classical Quantum Gravity **23**, 2129 (2006).
[58] C. Zhang, Reduced phase space quantization of black holes: Path integrals and effective dynamics, Phys. Rev. D **104**, 126003 (2021).
[59] K. Giesel, M. Han, B.-F. Li, H. Liu, and P. Singh, Spherical symmetric gravitational collapse of a dust cloud: Polymerized dynamics in reduced phase space, Phys. Rev. D **107**, 044047 (2023).
[60] K. Giesel and T. Thiemann, Scalar material reference systems and loop quantum gravity, Classical Quantum Gravity **32**, 135015 (2015).
[61] K. V. Kuchar and C. G. Torre, Gaussian reference fluid and interpretation of quantum geometrodynamics, Phys. Rev. D **43**, 419 (1991).
[62] V. Husain and T. Pawlowski, Time and a physical Hamiltonian for quantum gravity, Phys. Rev. Lett. **108**, 141301 (2012).
[63] T. Thiemann, Generalized boundary conditions for general relativity for the asymptotically flat case in terms of Ashtekar's variables, Classical Quantum Gravity **12**, 181 (1995).
[64] A. Corichi, I. Rubalcava, and T. Vukasinac, Hamiltonian and Noether charges in first order gravity, Gen. Relativ. Gravit. **46**, 1813 (2014).
[65] M. Campiglia, Note on the phase space of asymptotically flat gravity in Ashtekar–Barbero variables, Classical Quantum Gravity **32**, 145011 (2015).
[66] K. Giesel, S. Hofmann, T. Thiemann, and O. Winkler, Manifestly gauge-invariant general relativistic perturbation theory. I. Foundations, Classical Quantum Gravity **27**, 055005 (2010).
[67] M. Domagala, K. Giesel, W. Kaminski, and J. Lewandowski, Gravity quantized: Loop quantum gravity with a scalar field, Phys. Rev. D **82**, 104038 (2010).
[68] J. D. Brown and K. V. Kuchar, Dust as a standard of space and time in canonical quantum gravity, Phys. Rev. D **51**, 5600 (1995).
[69] P. Singh and E. Wilson-Ewing, Quantization ambiguities and bounds on geometric scalars in anisotropic loop quantum cosmology, Classical Quantum Gravity **31**, 035010 (2014).
[70] A. Ashtekar, J. Olmedo, and P. Singh, Quantum transfiguration of Kruskal black holes, Phys. Rev. Lett. **121**, 241301 (2018).
[71] A. Ashtekar and J. Olmedo, Properties of a recent quantum extension of the Kruskal geometry, Int. J. Mod. Phys. D **29**, 2050076 (2020).
[72] M. Assanioussi, A. Dapor, and K. Liegener, Perspectives on the dynamics in loop effective black hole interior, Phys. Rev. D **101**, 026002 (2020).
[73] R. Bousso, Charged Nariai black holes with a dilaton, Phys. Rev. D **55**, 3614 (1997).
[74] S. Hawking and S. F. Ross, Duality between electric and magnetic black holes, Phys. Rev. D **52**, 5865 (1995).
[75] P. Blanchard, R. Devaney, and G. Hall, *Differential Equations* (Cengage Learning, Boston, MA, 2012).
[76] A. Alonso-Bardaji, D. Brizuela, and R. Vera, An effective model for the quantum Schwarzschild black hole, Phys. Lett. B **829**, 137075 (2022).
[77] A. Alonso-Bardaji and D. Brizuela, Anomaly-free deformations of spherical general relativity coupled to matter, Phys. Rev. D **104**, 084064 (2021).
[78] A. Alonso-Bardaji and D. Brizuela, Nonsingular collapse of a spherical dust cloud, Phys. Rev. D **109**, 064023 (2024).

[79] K. Giesel, H. Liu, E. Rullit, P. Singh, and S. A. Weigl, Embedding generalized LTB models in polymerized spherically symmetric spacetimes, arXiv:2308.10949.

[80] K. Giesel, H. Liu, P. Singh, and S. A. Weigl, Generalized analysis of a dust collapse in effective loop quantum gravity: Fate of shocks and covariance, arXiv:2308.10953.

[81] F. Fazzini, V. Husain, and E. Wilson-Ewing, Shell-crossings and shock formation during gravitational collapse in effective loop quantum gravity, arXiv:2312.02032.

[82] V. Husain, J. G. Kelly, R. Santacruz, and E. Wilson-Ewing, On the fate of quantum black holes, Phys. Rev. D **106**, 024014 (2022).

[83] C. G. Callan, Jr. and F. Wilczek, On geometric entropy, Phys. Lett. B **333**, 55 (1994).